



HAL
open science

An eosimiid primate of South Asian affinities in the Paleogene of Western Amazonia and the origin of New World monkeys

Laurent Marivaux, Francisco R Negri, Pierre-Olivier Antoine, Narla S Stutz, Fabien L Condamine, Leonardo Kerber, François Pujos, Roberto Ventura Santos, André M V Alvim, Annie S Hsiou, et al.

► To cite this version:

Laurent Marivaux, Francisco R Negri, Pierre-Olivier Antoine, Narla S Stutz, Fabien L Condamine, et al.. An eosimiid primate of South Asian affinities in the Paleogene of Western Amazonia and the origin of New World monkeys. *Proceedings of the National Academy of Sciences of the United States of America*, 2023, 120 (28), pp.e2301338120. 10.1073/pnas.2301338120 . hal-04153825

HAL Id: hal-04153825

<https://hal.science/hal-04153825v1>

Submitted on 6 Jul 2023

HAL is a multi-disciplinary open access archive for the deposit and dissemination of scientific research documents, whether they are published or not. The documents may come from teaching and research institutions in France or abroad, or from public or private research centers.

L'archive ouverte pluridisciplinaire **HAL**, est destinée au dépôt et à la diffusion de documents scientifiques de niveau recherche, publiés ou non, émanant des établissements d'enseignement et de recherche français ou étrangers, des laboratoires publics ou privés.

An eosimiid primate of South Asian affinities in the Paleogene of Western Amazonia and the origin of New World monkeys

Laurent Marivaux^{a,*}, Francisco R. Negri^b, Pierre-Olivier Antoine^a, Narla S. Stutz^{a,c}, Fabien L. Condamine^a, Leonardo Kerber^d, François Pujos^e, Roberto Ventura Santos^f, André M. V. Alvim^f, Annie S. Hsiou^g, Marcos C. Bissaro Júnior^g, Karen Adami-Rodrigues^h, and Ana Maria Ribeiro^{c,i}

^aLaboratoire de Paléontologie, Institut des Sciences de l'Évolution de Montpellier (ISE-M, UMR 5554, CNRS/UM/IRD), Université de Montpellier (UM), Place Eugène Bataillon, 34095, Montpellier, France

^bLaboratório de Paleontologia, Campus Floresta, Universidade Federal do Acre, Estrada do Canela Fina, Km 12, 69980-000, Cruzeiro do Sul, Acre, Brazil

^cPrograma de Pós-Graduação em Geociências, Universidade Federal do Rio Grande do Sul, Av. Bento Gonçalves 9500, 91501-970, Porto Alegre, Rio Grande do Sul, Brazil

^dCentro de Apoio à Pesquisa Paleontológica da Quarta Colônia (CAPP), Universidade Federal de Santa Maria, R. Maximiliano Vizzotto 598, 97230-000, São João do Polêsine, RS, Brazil

^eInstituto Argentino de Nivología, Glaciología y Ciencias Ambientales (IANIGLA), CONICET–UNCUYO–Mendoza, Avenida Ruiz Leal s/n, Parque Gral. San Martín, 5500, Mendoza, Argentina

^fLaboratório de Geocronologia, Instituto de Geociências, Universidade de Brasília (UnB), Campus Universitário Darcy Ribeiro ICC - Ala Central, 70910-000, Brasília, Distrito Federal, Brazil

^gLaboratório de Paleontologia, Universidade de São Paulo, Av. Bandeirantes 3900, 14040-901, Ribeirão Preto, São Paulo, Brazil

^hNúcleo de Estudos em Paleontologia e Estratigrafia, Centro das Engenharias, Universidade Federal de Pelotas, R. Benjamin Constant 989, 96010-020, Pelotas, Rio Grande do Sul, Brazil

ⁱSeção de Paleontologia, Museu de Ciências Naturais, Secretaria do Meio Ambiente e Infraestrutura, Av. Dr. Salvador França 1427, 90690-000, Porto Alegre, Rio Grande do Sul, Brazil

*To whom correspondence may be addressed (Laurent.Marivaux@UMontpellier.fr)

Author Contributions: AMR, FRN, POA, and LM designed research; FRN, AMR, POA, LM, LK, FP, NSS, RVS, AMVA, ASH, MCBJ, and KAR performed research and fieldwork; LM, FLC, NSS, and LK analyzed data; LM wrote the paper; and POA, FLC, NSS, FP, ASH, AMVA, RVS, and AMR reviewed the manuscript and provided edits.

Competing Interest Statement: The authors declare no competing financial interests.

Classification: Biological Science - Evolution.

Keywords: Brazilian Amazonia, Basal Anthrozoidea, Platyrrhini, Teeth, Phylogeny, Paleobiogeography.

Abstract. Recent fossil discoveries in Western Amazonia revealed that two distinct anthropoid primate clades of African origin colonized South America near the Eocene/Oligocene transition (*ca.* 34 Ma). Here we describe a diminutive fossil primate from Brazilian Amazonia and suggest that, surprisingly, a third clade of anthropoids was involved in the Paleogene colonization of South America by primates. This new taxon, *Ashaninkacebus simpsoni* gen. et sp. nov., has strong dental affinities with Asian-African stem anthropoids: the Eosimiiformes. Morphology-based phylogenetic analyses of early Old World anthropoids and extinct and extant New World monkeys (platyrrhines) support relationships of both *Ashaninkacebus* and *Amamria* (late middle Eocene, North Africa) to the South Asian Eosimiidae. Afro-Arabia, then a mega-island, played the role of a biogeographic stopover between South Asia and South America for anthropoid primates and hystricognathous rodents. The earliest primates from South America bear little adaptive resemblance to later Oligocene-early Miocene platyrrhine monkeys, and the scarcity of available paleontological data precludes elucidating firmly their affinities with or within Platyrrhini. Nonetheless, these new data shed light on some of their life-history traits, revealing a particularly small body size and a diet consisting primarily of insects and possibly fruit, which would have increased their chances of survival on a natural floating island during this extraordinary over-water trip to South America from Africa. Divergence-time estimates between Old and New World taxa indicate that the transatlantic dispersal(s) could source in the intense flooding events associated with the late middle Eocene climatic optimum (*ca.* 40.5 Ma) in Western Africa.

Significance Statement Western Amazonia has recently revealed that two distinct anthropoid primate clades of African origin colonized South America near the Eocene/Oligocene transition (*ca.* 34 Ma). Here we report a new fossil primate from Brazilian Amazonia pointing to a third clade involved in that colonization. Surprisingly, this taxon has strong affinities with eosimiid anthropoids of South Asian origin. These new data highlight some of the life-history traits (very small-bodied-size and insectivory/frugivory) that would have increased the chances of survival on a natural raft during this extraordinary transatlantic journey from Africa to South America. Estimated splits between New and Old World taxa indicate that the dispersal(s) coincide with the late middle Eocene climatic optimum (*ca.* 40.5 Ma), which generated intense flooding events.

Introduction

Reconstructing the origins, historical biogeography, and early evolutionary histories of Neotropical platyrrhine primates and caviomorph rodents has long been among the most attractive and challenging issues in (paleo-)mammalogy. These two groups are parts of those Asian-African mammal clades (Anthropoidea and Hystricognathi, respectively), which appeared in the South American fossil record by mid-Cenozoic times. Thanks to a significant set of morphological and molecular evidence assembled over more than half a century, both groups are conjectured to have migrated across the South Atlantic Ocean from Africa to South America (1–10).

Recent paleontological efforts in the Paleogene of Western Amazonia, especially in the Andean foothills of Peru, have provided fundamental new information on the early primates and rodents of South America (8, 11–20). In particular, they have shed new light on their phylogenetic affinities with coeval late Eocene/early Oligocene African relatives, and thus refined the timeframe for the colonization(s) of South America by both groups, which is consistent with estimates derived from molecular clock phylogenies (7, 9, 10, 21, 22). However, the pattern of colonization, notably for primates, turns out to be more complex than previously thought since the recent discoveries in Peruvian Amazonia (*Perupithecus* Bond et al., 2015 and *Ucayalipithecus* Seiffert et al., 2020) reveal a polyphyletic colonization of South America by anthropoids of African origin. Along with the African hystricognath ancestor of caviomorph rodents, at least two basal anthropoid clades known in Africa (Oligopithecidae-like primates and Parapithecidae) colonized South America at the end of the Eocene epoch or near the Eocene/Oligocene transition (EOT), presumably via sweepstakes transatlantic dispersals (floating island rafting) (8, 12, 19). However, paleontological evidence remains scarce to comfort this biogeographic scenario.

Here we report the discovery of a new fossil primate from Brazilian Amazonia (*Rio Juruá*, State of Acre). Although the taxon is documented by a single isolated tooth, it points to a third clade of basal anthropoids involved in the Paleogene colonization of South America by primates. This discovery provides increasingly puzzling insights into the origin and historical biogeography of New World monkeys, as the new taxon, *Ashaninkacebus simpsoni* gen et sp. nov., has strong affinities with stem anthropoid primates not of African but of South Asian origin: the Eosimiidae.

Results

Systematic Paleontology. Order Primates Linnaeus, 1758; Suborder Anthropoidea Mivart, 1864; Family Eosimiidae Beard, Qi, Dawson, Wang and Li, 1994.

***Ashaninkacebus simpsoni* gen. et sp. nov.**

Etymology. Generic name refers to “*Asháninka*”, a native ethnic group living in the rainforests of Western Amazonia, in Brazil (*Rio Juruá*, Acre) and more widely in Peru (*Río Alto Yurúa*, Ucayali, up to the watershed of the Peruvian Andes), with the Ancient Greek suffix κῆβος (*kêbos* = *cebus*), i.e., long-tailed monkey. Epithet in honor of the renowned evolutionary paleontologist George Gaylord Simpson, who co-led a joint Brazilian-American Museum paleontological expedition to the *Rio Juruá* in 1956. In recognition of the many fossil-bearing sites he discovered on this trip, but also for his courage after an accident he suffered on this river that almost cost him his life.

Holotype. UFAC-CS 066, right upper M1 (Fig. 1A–E); the fossil is permanently housed in the collections of the Paleontology Laboratory of the *Universidade Federal do Acre* (UFAC), Floresta campus, Cruzeiro do Sul (CS), Acre, Brazil.

Type Locality. *Ponto Rio Juruá* n°33' (PRJ-33'), situated on the left bank of the *Rio Juruá* (*Alto Yurúa*), 1 km upstream from the junction with the *Rio Breu* and the small village of *Foz do Breu*, Acre, Brazil (*SI Appendix, Fig. S1*).

Comments. The UFAC-CS 066 fossil specimen was recovered in allochthonous detrital Holocene sediments (PRJ-33', fine sand mixed with transported blocks of microconglomerate) deposited directly beneath the *in situ* PRJ-33 fossil-bearing locality, the latter being late middle Miocene in age, including the caviomorph rodents *Microscleromys* sp. (Chinchilloidea) and *Nuyuyomys* sp. (Erethizontoidea), both genera recognized in the Laventan South American Land Mammal Age (SALMA) at La Venta, Colombia, and TAR-31, Peru (23, 24). The precise upriver provenance and stratigraphic context of the UFAC-CS 066 primate tooth reported from PRJ-33' remain unknown. However, isolated teeth of caviomorph rodents documenting *Eoincamys* sp. [sp. 1] (25) as well as *Cachiyacuy* sp. [sp. 2] were found in the same PRJ-33' allochthonous primate-yielding sediments (*SI Appendix, Fig. S2*), thereby indicating a Paleogene age, likely around the Eocene/Oligocene transition (EOT; i.e., *ca.* 34 Ma). These rodent genera are documented from several Peruvian fossil-bearing localities, notably from the geographically-close Santa Rosa locality (*Alto Yurúa*, Ucayali [sp. 1+2]) (11, 18, 20), early Oligocene in age (26), from the Shapaja localities crossing the EOT (*Ríos Huallaga/Mayo*,

San Martín [sp. 1]) (15, 27), and from some of the Contamana localities considered as preceding the EOT (*Quebrada Cachiyacu*, Loreto [sp. 2]) (8, 14, 28).

Age. Nearby the Eocene/Oligocene transition (i.e., *ca.* 34 Ma), deriving from biochronological inferences. This temporal frame is independently corroborated by the median age estimate for *Ashaninkacebus* (≈ 32.9 Ma, 95% highest posterior density [HPD] = 42.1–19.9 Ma) deriving from a Bayesian tip-dating analysis performed with a morphology-based phylogeny of basal anthropoid primates (+ extinct and extant Platyrrhini; see below Fig. 2).

Diagnosis (based on the Holotype). Small-sized primate having upper molars low-crowned, transversely elongated, with a distal crown margin markedly invaginated, and primarily tritubercular with acute paracone, metacone and protocone, associated with a set of well-defined and sharp transverse and longitudinal crests (long and U-shaped pre- and post-protocone cristae, long hypoparacrista, short hypometacrista combined with a metacrista [= hypometacrista complex], and buccal shearing crests forming a long and complete eocrista); presence of a minute, not cusped hypocone on a strong distolingual cingulum; buccal crown margin bearing a complete buccal cingulum, particularly expanded at the level of the metacone, and including a well-defined metastylar shelf; no appreciable development of conules and parastyle (the dental terminology used here is presented in [SI Appendix, Fig. S3](#)).

Differential Diagnosis (with Paleogene eosimiiform anthropoids). *Ashaninkacebus* differs from known Asian eosimiids, especially *Eosimias centennicus*, *Phenacopithecus krishtalkai* (middle Eocene, China) and *Bahinia banyueae* (early Oligocene, China) in being smaller, having a less angular and more smoothly rounded metastylar shelf, and in showing a quasi-non-development of the parastyle. It further differs from *P. krishtalkai*, but also from *Bahinia pondaungensis* (late middle Eocene, Myanmar) in being clearly smaller, displaying a lesser development of the mesial cingulum, lacking the entoprotocrista, and in having a buccal cingulum that is less developed and less extended buccomesially. Differs more particularly from *B. pondaungensis* in having a distal crown margin of the molar much more invaginated, displaying much less bulbous cusps, a lesser development of the hypometacrista complex, in lacking the development of an endoprotocrista in the trigon basin, and in showing a better development of the distolingual cingulum, which bears a minute hypocone. With the latter character condition, *Ashaninkacebus* also differs markedly from *B. banyueae* and *E. centennicus*. Differs from *Amamria tunisiensis* (late middle Eocene, Tunisia) in displaying a waisted rather than straight distal crown margin, in having a less pronounced shelf of the buccal cingulum, especially at the mesiobuccal corner of the crown, a more discrete mesial cingulum without pericone, stronger hypoparacrista

and hypometacrista complex delimiting with the pre- and post-protococone cristae a more extensive trigon basin, and in displaying a cingular not cusped hypocone. Differs from known Afro-Asian afrotarsiids (*Afrotarsius libycus* and *Afrasia djijidae*; late Eocene of Libya and late middle Eocene of Myanmar, respectively) in lacking the conules and, more especially, the postmetaconule crista (prominently developed on the M2 of *Afrasia* and *Afrotarsius*, but not on the M1 of *Afrasia*), in displaying a complete and continuous lingual cingulum with the development in the distolingual part of a minute hypocone (absent in afrotarsiids), and in having a more buccally extensive distal cingulum that reaches the base of the metastylar shelf, whereas it is limited near the midline of the crown in afrotarsiids (at least on the M2 of *Afrotarsius* and *Afrasia*, but not on the M1 of *Afrasia*). Differs more specifically from *Afrasia* in lacking the strong development of the parastyle in buccal position with respect to the paracone, and in showing a stronger development of the hypoparacrista and hypometacrista complex. *Ashaninkacebus* differs from *Phileosimias* (*P. kamali* and *P. brahuiorum*; early Oligocene, Pakistan) in lacking the conules, in having a stronger development of the lingual cingulum, a more invaginated distal margin, and in developing hypoparacrista and hypometacrista (both crests being absent in *Phileosimias*).

Description. A detailed description is provided in [SI Appendix, Text S1](#) (see also [SI Appendix, Fig. S4](#)).

Comparisons (with relevant simiiform anthropoids, including platyrrhines). *Ashaninkacebus* exhibits a suite of characters on the upper molar, which are primarily found in eosimiiform anthropoids. Some of these characters, such as the development of the buccal cingulum, the presence of a pronounced metastylar shelf (deriving from a buccal position of the metastyle with respect to the metacone and the presence of a long postmetacrista) are dental specializations of eosimiiforms, whereas some other characters, such as the deep invagination of the distal crown margin and the absence or weak development of a hypocone (cingular or cusped hypocone but in the latter case remaining a very small tubercle) may be viewed as primitive (i.e., symplesiomorphies) compared to the dental patterns characterizing simiiform anthropoids. *Ashaninkacebus* appears somewhat as a morphological intermediate, at least based on the limited morphological information in the only available specimen, a single upper molar (M1). This intermediate status is suggested by the presence of a cingular hypocone (i.e., incipient development of a hypocone) and in the tendency to reduce the buccal cingulum and the metastylar shelf.

Ashaninkacebus differs from its South American companion, *Perupithecus ucayaliensis* (early Oligocene, Santa Rosa, Peru), in preserving the buccal cingulum and metastylar shelf (which are strongly reduced if not almost absent in *Perupithecus*, thereby placing its buccal

cusps in a marginal position, with steep buccal flanks), in having a much higher degree of invagination of the distal crown margin, in lacking the entoprotocrista, and in displaying a weaker development of the hypoparacrista and hypometacrista complex. The M1 of *Ashaninkacebus* is also more transversely shaped, with a narrower trigon basin (i.e., narrow U-shaped pre- and post-protocone cristae, as in several other eosimiiforms). In contrast, in *Perupithecus*, as well as in North African oligopithecids, proteopithecids, parapithecids and propliopithecids, some South Asian amphipithecids, and in stem and crown South American platyrrhines, upper molars are more quadrangular-shaped, and their trigon basins are remarkably widened and vast in several cases (i.e., wider/flat U-shaped pre- and post-protocone cristae, with notably a more distally directed postprotocrista). On the other hand, the two unassigned tooth fragments (trigons of two upper molars; CPI-7000 and CPI-7001) found in association with *Perupithecus* in Santa Rosa (ref. 12, their figure 3C–D) present interesting characteristics, being roughly similar both in size and morphology to the lingual region of the M1 of *Ashaninkacebus*. These lingual tooth fragments bear a small and limited-in-length mesial cingulum, and a lingual cingulum that widens in its distal region (notably on CPI-7000, much less on CPI-7001), suggesting the presence of a cingular hypocone but much less pronounced than on UFAC-CS 066 of *Ashaninkacebus*. The distal region of CPI-7000 is better preserved than in CPI-7001, and reveals a somewhat deep invagination of the distal crown margin, close to that characterizing UFAC-CS 066. CPI-7000 preserves parts of the lingual flanks of the paracone and metacone, which display roughly similar development of the hypoparacrista and of the hypometacrista complex connected to the postprotocrista, as described on UFAC-CS 066. Although the buccal regions, highly diagnostic for *Ashaninkacebus*, are not preserved on these two specimens from Santa Rosa, based on the characters of their lingual parts, it is not excluded that the diminutive taxon represented by these two half-teeth is very closely related to *Ashaninkacebus*.

The oligopithecid *Oligopithecus rogeri* (early Oligocene, Oman) displays upper molars with a strong invagination of their distal crown margins, among the deepest observed in basal anthropoids, and does not show any development of a hypocone on the strong distolingual cingulum. In contrast, its closest relative, *Catopithecus browni* (latest Eocene, Egypt), has upper molars with a very weak invagination of their distal margins, as seen in *Perupithecus*, but unlike the latter, upper molars bear a small but well-defined and cusped hypocone on their distolingual cingulum. The same applies to the proteopithecine parapithecid *Proteopithecus sylviae* (latest Eocene, Egypt), documented by upper molars with a more rectangular crown outline, without any distal invagination, and with the development of a distolingual hypocone. In most other basal simiiforms, including stem and crown platyrrhines (except callitrichine cebids), the quadrangular crown outline,

without distal invagination, is mainly related to the development of the hypocone, which can become, in several cases, a full-fledged tubercle, as large as the three other main cusps.

Catopithecus and *Proteopithecus* display a moderately developed to discrete buccal cingulum on upper molars, whereas *Oligopithecus*, as *Perupithecus*, shows almost no development of the buccal cingulum or only a trace of it, a condition that is distinct from that of the eosimiiforms, and, in particular, *Ashaninkacebus*. Furthermore, in all these previous African taxa plus *Perupithecus*, there is no development of a prominent metastylar shelf as observed in eosimiiforms and *Ashaninkacebus*. A buccal cingulum may also be noticed in some Eocene and Oligocene African parapithecids (e.g., *Biretia*, *Apidium*, and *Simonsius*) and some South Asian amphipithecids (e.g., *Ganlea*, *Myanmarpithecus*, *Bugtipithecus*, and *Pondaungia*). However, this dental trait appears in these taxa most often as a trace, a vestige, or in most cases, it is limited between the two buccal cusps. It is never as buccally extensive as in eosimiiforms.

The development of a buccal cingulum is hardly ever observed in the upper molars of both basal and more advanced (crown) platyrrhines of South America. At most, this cingulum occurs as a vestige in a very small number of basal taxa (*Parvimico* and *Mazzonicebus*; early Miocene, Peru and Argentina, respectively). In most platyrrhines (except several callitrichines), the buccal cusps are bulbous and their buccal flanks are generally steep-sided, without buccal cingulum (cusps positioned marginally). However, a few cases of buccal cingulum are observed in some large platyrrhine taxa (e.g., *Alouatta*, *Stirtonia*, and *Paralouatta*), seemingly secondarily acquired and linked to a specialized diet (folivory). Some modern platyrrhines (e.g., ateline atelids, and certain pitheciine pitheciids such as *Cacajao* and *Chiropotes*, or even the callicebine pitheciid *Xenothrix* from the Quaternary of Jamaica), in addition to lacking a buccal cingulum, also lack a lingual cingulum, despite the development of a strong hypocone. Most platyrrhines (except several callitrichines) are medium to large-sized, and have quadritubercular upper molars with bulbous cusps. They also show a wide range of variations in the development (length and thickness) or non-development of the buccal transverse crests (hypoparacrista and hypometacrista complex), and in the connection of the latter with the pre- and post-protocone cristae (the latter also showing a different degree of development). These dental conditions and variations correspond to specializations over time to specific diets (incidentally also associated with body-size changes); therefore, they are not directly comparable to the primitive dental pattern of small-bodied extinct species such as *Ashaninkacebus*, and even *Perupithecus*. Comparisons with small-bodied callitrichine cebids are certainly more relevant, although callitrichines also show dental specializations.

Callitrichines are somewhat peculiar among platyrrhines, not only by their small body size, but also by their dental transformations/specializations, which led, among other things, to a strong reduction of the toothrow length and the loss in some taxa of the third molar (*Callithrix*, *Mico*, *Cebuella*, *Saguinus*, and *Leontopithecus*), associated with a reconfiguration of the second molar occlusal pattern and crown outline. Compared to the M1 of *Ashaninkacebus*, which is rather transversely arranged and distally waisted, callitrichines have a more triangular-quadrangular M1, with paracone and metacone slightly more distant from each other, and with very little or no (*Cebuella* or the extinct *Lagonimico* from the late middle Miocene, Colombia) distal invagination of the crown. The lingual cingulum may be either strongly developed (*Lagonimico*, *Leontopithecus*, and *Callimico*), weakly developed (some species of *Callithrix/Mico*), or vestigial to absent (*Cebuella* and some species of *Callithrix/Mico*). When present, the lingual cingulum very rarely bears a hypocone in its distal region, as it does in *Ashaninkacebus* (cingular hypocone). Upper molars of some callitrichines (except in *Callimico*, *Leontopithecus*, and *Cebuella*) display a kind of buccal cingulum, which can be described as a mesiodistally-extended enamel bulge (embedding the swollen bases of the paracone and metacone), rather than a full-fledged enamel shelf/fold. Unlike *Ashaninkacebus* and eosimiiforms in general, callitrichines have no metastyle or can display only a small enamel swelling, which is in line with the paracone-metacone axis. The postmetacrista is mostly absent or very weak, low and short when present, and there is no postmetacrista-metastylar shelf structure contrary to what is observed in *Ashaninkacebus* and eosimiiforms. In contrast, the distal cingulum can be much more buccally extensive than in eosimiiforms (or other basal anthropoids and several other platyrrhines), running at the base of the crown and surrounding the distobuccal aspect of the metacone. This condition is evident in several species of *Callithrix/Mico* and in *Cebuella* (as well as in *Parvimico*; early Miocene, Peru), in which the postmetacrista is very weakly developed or absent. A noticeable character of differentiation is the strong development of the hypoparacrista in *Ashaninkacebus*, whereas this crest is absent in callitrichines, and as such, the lingual flank of the paracone is free-standing and steep-sided in the latter. The absence or very weak development (very low and/or extremely short) versus long and strong development of the hypoparacrista is variably distributed among platyrrhines. If this crest is particularly strong, long and trenchant in *Perupithecus*, most stem platyrrhines (in late Oligocene *Canaanimico* and *Branisella*, and early Miocene *Homunculus*, *Carlocebus*, *Soriacebus*, *Mazzonicebus*, and *Dolichocebus*) and in certain cebine and aotine cebids (*Panamacebus*, *Cebus/Sapajus*, *Acrecebus*, and *Aotus*), it is variably present in *Saimiri* and *Neosaimiri* (cebinés), very weak to absent in extinct and extant pitheciids, and absent in extinct and extant atelids, Quaternary West Indian *Antillothrix* and *Paralouatta*, and in *Parvimico*. As in

Ashaninkacebus, the hypometacrista is also weakly developed and very short (or often absent) in callitrichines. Finally, as in *Ashaninkacebus*, callitrichines (and all other platyrrhines) display a well-developed distal metacrista, which may or may not be lingually connected to the postprotocrista. The latter is long and runs buccally in *Ashaninkacebus*, whereas it is variable in length and more distally directed in callitrichines (and platyrrhines in general).

Body Mass Estimates. Adult body mass of *Ashaninkacebus simpsoni* is estimated at 228–231 g on the basis of the M1 area (5.9276 mm²), by using the two regression equations provided by Egi et al. (29) (see Methods). This taxon was a diminutive primate with a body mass much inferior to that estimated for the platyrrhine ancestral condition derived from comparative phylogenetic methods [i.e., ~400 g (30)]. *Ashaninkacebus* was about the size of some small living marmoset callitrichines [e.g., *Callithrix jacchus*, 236–256 g after Ford (31) or 317–324 g after Smith and Jungers (32); or *C. penicillata*, 182–225 g after Ford (31) or 307–344 g after Smith and Jungers (32)], nonetheless it was larger than the pygmy marmoset [*Cebuella pygmaea*, 126–130 g after Ford (31) or 110–122 g after Smith and Jungers (32)]. It was also likely of the same size as the extinct platyrrhine *Parvimico materdei* from lower Miocene deposits of Madre de Dios, Peru [235–239 g (33)] and slightly smaller than the South Asian eosimiid *Eosimias centennicus* (~250 g) and afrotarsiid *Afrasia djijidae* (~270 g) from the middle Eocene of China and Myanmar, respectively (34, 35). *Ashaninkacebus* was otherwise one-third smaller than *Perupithecus ucayaliensis* (477–494 g) from the early Oligocene Santa Rosa locality (Peru), the body mass of which was more roughly close to that of some small living tamarin callitrichines [e.g., *Saguinus nigricollis*, 470–480 g after Ford (31) or 468–484 g after Smith and Jungers (32)]. *Ashaninkacebus* was also smaller-bodied than *Ucayalipithecus perdita* from Santa Rosa, whose body size was estimated to be close to that of a medium-sized marmoset callitrichine [319–366 g (19)].

M1 Shearing Quotient (SQ) and Diet Reconstruction. Measurement of the M1 buccal cutting-edge development of *Ashaninkacebus* (see Methods) reveals a positive and high SQ value (= 16.62), thereby reflecting well-developed shearing crests. Compared to platyrrhines with medium to small body masses (less than 1 kg; ref. 33, their figure 6B), the relatively high SQ and the very small body size of *Ashaninkacebus* indicate a diet with primarily insect and probably fruit consumption, but lacking exudates and leaves.

Phylogenetic Analyses. We performed a cladistic assessment of the morphological evidence (A1 analysis) to investigate the phylogenetic position of *Ashaninkacebus* in a high-level phylogeny of basal anthropoids from the Old World (i.e., Paleogene South Asian and North African known taxa), plus known extinct and extant New World platyrrhines (*S*

[Appendix, Table S1](#)). The data matrix included 456 characters and 81 taxa (see Methods for character assumptions, data, and phylogenetic analyses; also, [SI Appendix, Table S2 and Text S2](#)). We enforced a molecular backbone tree on the dataset to recover extant primate clades strongly supported by genomic sequences (see Methods). The analyses yielded a single most-parsimonious tree (2429.49 steps, Consistency index = 0.36; Retention index = 0.56; Fig. 2; [SI Appendix, Fig. S5](#)). These results show that the three oldest known primates from the early Oligocene of South America are not related to later platyrrhine monkeys but are nested within three distinct clades of Old World basal anthropoids (Fig. 2). *Ashaninkacebus* is nested within the Eosimiidae clade (sister to *Bahinia*), *Perupithecus* within the Oligopithecidae clade (sister to *Talahpithecus*), and *Ucayalipithecus* is nested within the Parapithecidae clade (sister to *Qatrania*) as formerly resolved by Seiffert et al. (19). Within Platyrrhini, we recover a pattern underscoring a stem radiation *versus* crown radiation (36, 37), with, however, some changes regarding the Pleistocene Caribbean taxa (*Antillothrix/Insulacebus*, *Paralouatta*, and *Xenothrix*). The latter were previously resolved as stem platyrrhines (13, 37), but are interpreted here as crown platyrrhines. For the analysis, we have constrained the phylogenetic position of *Xenothrix* close to the Callicebinae, inasmuch as ancient DNA analyses recently demonstrated its pitheciid affinities (38). In contrast, *Paralouatta* and *Antillothrix/Insulacebus*, along with *Parvimico* and *Chilecebus*, are here resolved as a sister clade to the Atelidae, or stem Atelidae [as originally proposed for *Paralouatta* (39)], but see Kay et al. (33) for different results regarding these aforementioned taxa. These results may seem somewhat surprising in view of the phylogenetic position of the Paleogene South Asian Amphipithecidae, which branch quite high in the Anthropeida clade, being resolved close to the Catarrhini clade, and as sister to Platyrrhini. However, this relationship is not strongly supported (Bremer support of 1; [SI Appendix, Fig. S5](#)), relying on a few morphological characters, possibly convergent (see [SI Appendix, Text S3](#)). In this phylogenetic context, constraining the Amphipithecidae in a more basal position within the Anthropeida clade [i.e., stem anthropoids, diverging after the Eosimiiformes (19, 40); A2 analysis] requires 12 additional steps (see [SI Appendix, Fig. S6](#)).

The phylogenetic topology obtained by maximum parsimony (A1) was then subjected to a Bayesian tip-dating (BTD) analysis, for the sole purpose of estimating divergence times between taxa (see Methods; [SI Appendix, Table S2 and Text S2](#)). All nodes of the age-free cladogram were applied as hard constraints for the BTD analysis (A3). We duplicated this BTD analysis in enforcing the topology considering the Amphipithecidae in a more basal position (A4). *Ashaninkacebus* was assigned to a broad age prior to these analyses since its stratigraphic context is unknown (see Methods). The BTD analyses returned a median age of ≈ 32.9 Ma (95% HPD = 42.1–19.9 Ma) for this new taxon, an age that is consistent with

the biochronological inferences derived from the caviomorph rodents found in association at PRJ-33' (i.e., nearby the Eocene/Oligocene transition, *ca.* 34 Ma). Also of interest are the divergence-time estimates of the three ancient primates found in South America from their Old World counterparts, estimates which can be traced back to the late middle–late Eocene for *Perupithecus* (≈ 37.33 Ma, 95% HPD = 40.3–35.3 Ma), to the late middle Eocene–earliest Oligocene for *Ucayalipithecus* (≈ 35.93 Ma, 95% HPD = 40.6–32.0 Ma), and to the middle–late Eocene for *Ashaninkacebus* (≈ 41.8 Ma, 95% HPD = 45.5–38.9 Ma) (Fig. 2; see also [SI Appendix, Fig. S7, Tables S3 and S4](#)). It is worth mentioning the somewhat old age estimates derived from our BTM analysis (i.e., morphological clock analysis) regarding the emergence of the three main crown Platyrrhini families (Pitheciidae, Atelidae, and Cebidae), compared to molecular-based estimates (21, 22). Although older ages are expected under a BTM approach (41), our age estimates can be inflated using morphological and/or morpho-paleontological data alone, without molecular data, since morphology does not evolve in the same "clock-like" manner as molecules (42, 43). Here, the crown platyrrhine radiation is traced back to the early Oligocene, resulting in a substantial incompleteness of the fossil record, while the stem platyrrhine radiation is estimated to extend back to the late middle Eocene ([SI Appendix, Table S4](#)). The latter estimates coincide to some extent with the divergence-time estimates of the three ancient South American primate fossils from their Old World counterparts, although no phylogenetic relationship can be formally established between *Ashaninkacebus* or *Perupithecus* and the stem platyrrhines yet (see Discussion). Note that a basal placement of the Amphipithecidae clade (A4) has virtually no effect on the morphological clock analysis for estimating divergence times between taxa ([SI Appendix, Fig. S8, Table S4 and Text S3](#)).

Finally, we estimated simultaneously phylogenetic topology and divergence times of taxa in performing a partially constrained BTM analysis (A5), which enforced only the molecular backbone tree of living species and the topology of the branching groups of Anthropeidea plus outgroups as resolved in A1 (see Methods; [SI Appendix, Table S2](#)). Despite some phylogenetic changes regarding a few taxa, this analysis did not result in conflicting topologies compared to the results of the parsimony analyses ([SI Appendix, Fig. S9 and Text S3](#)). The three oldest known primates from the early Oligocene of South America are also found here nested within the same three distinct clades of Old World basal anthropoids. *Ashaninkacebus* is resolved here as the earliest offshoot of the Eosimiidae clade among the Eosimiiformes. Its stemward phylogenetic position within the Eosimiidae affects the estimate of its median age, which is set back more than 6 million years (≈ 38.8 Ma; 95% HPD = 45.0–25.8 Ma; [SI Appendix, Table S4](#)). Such an old age is otherwise inconsistent with the biochronological inferences assembled from PRJ-33'.

Besides, the divergence-time estimate of *Ashaninkacebus* from other eosimiids is incredibly old (≈ 49.3 Ma; 95% HPD = 53.4–45.3 Ma; [SI Appendix, Table S4](#)) and somewhat unlikely (see our complementary discussion; [SI Appendix, Text S3](#)). From this BTD analysis (A5), the crown and stem platyrrhine radiations are estimated to have occurred slightly more recently than previously found in the A3 analysis ([SI Appendix, Table S4](#)), but still implying a substantial incompleteness of the platyrrhine fossil record. Outside of the Platyrrhini clade, this BTD analysis (A5) recovers the crownward branching of the Amphipithecidae within the Anthroidea clade ([SI Appendix, Fig. S9](#)). Applying a stemward constraint on the branching of the Amphipithecidae (A6; [SI Appendix, Fig. S10](#)) did not impact the rest of the topology or the divergence-time estimates ([SI Appendix, Table S4 and Text S3](#)).

All these analyses (parsimony and the multiple BTD analyses) returned identical results regarding the eosimiid status of the new taxon *Ashaninkacebus*. Finally, we examined the uncertainty of the phylogenetic position of *Ashaninkacebus* across the posterior trees of the BTD analyses (A5 and A6), using the RoguePlots approach (44). In these two BTD analyses, *Ashaninkacebus* was always recovered nested within the Eosimiiformes ([SI Appendix, Figs. S11 and S12](#)).

Discussion

Macroevolutionary Implications. The oldest known primates from South America are so far represented only by a few isolated teeth, documenting three clearly distinct species: either much more primitive (*Perupithecus* and *Ashaninkacebus*) or radically different/specialized (*Ucayalipithecus*) with respect to any known platyrrhines. As a result, none of these earliest South American anthropoid taxa is related to later platyrrhine monkeys (Fig. 2). *Perupithecus* was previously recovered at the root of Platyrrhini (19, 33, 43), but from phylogenetic analyses made with a much more restricted taxonomic sampling, *i*) excluding poorly known African Eocene taxa of utmost evolutionary interest, such as *Talahpithecus* and *Amamria*, and *ii*) lacking a comprehensive sampling of early-diverging anthropoids from the Paleogene of both Africa and Asia (33, 43). *Ucayalipithecus* is diverging and highly specialized compared to *Perupithecus*, *Ashaninkacebus* and known basal platyrrhines. Its dental specialization (bulbous cusps, conules, styles, cuspids and stylids, with limited crests and cristids; i.e., bunodonty) is similar to that of its coeval African parapithecoid counterparts [i.e., primary frugivorous (19, 45)]. Such a specialization could have been selectively advantageous in the short term after the arrival of its lineage in South America,

but ultimately resulted in low diversification, further leading to its extinction without leaving any extant relatives (i.e., evolutionary dead end). The very small-bodied *Ashaninkacebus* and slightly larger *Perupithecus* have teeth much more crested (notably marked buccal shearing crests) and with acute cusps, indicating a mixed diet including primarily insects and also fruit [high SQ values; our results and those of Kay et al. (33)]. These two taxa are intriguing because they harbor dental patterns strikingly similar to those of some basal anthropoids such as South Asian eosimiids and African oligopithecids-like primates, respectively, but not to those of any known South American stem platyrrhines (late Oligocene and early Miocene in age). This raises the question of whether we should consider the dental patterns of *Ashaninkacebus* and *Perupithecus* to be highly convergent with those of these Old World basal anthropoids. From our assessment of the current dental evidence, they are interpreted as supporting phylogenetic affinities (Fig. 2). Insofar as the three oldest primates known to date in South America are nested in either African or South Asian clades, but not at the root of Platyrrhini, should we consider that we have not yet found a close relative of the platyrrhine ancestor? Should we also draw the conclusion of evolutionary dead ends for the lineages of *Ashaninkacebus* and *Perupithecus*? It is likely premature to answer these questions. Indeed, when analyzing evolutionary trends regarding upper molar character transformations over time within Anthropeida or even in the closest outgroups of anthropoids (e.g., extinct tarsiiforms and adapiforms, extinct and extant strepsirrhines), the morphological changes from primitive dental structures characterizing *Ashaninkacebus* or *Perupithecus* towards derived structures observed in some early platyrrhines, such as *Dolichocebus*, *Homunculus*, *Carlocebus*, *Mazzonicebus*, *Canaanimico* or *Parvimico*, are not structurally unrealistic (e.g., development of more bulbous cusps, increased size of the hypocone with a more quadrangular outline of the crown, more developed crests in several cases). In other words, the dental patterns of *Ashaninkacebus* or *Perupithecus* could match the expected ancestral platyrrhine dental condition. That *Perupithecus* or *Ashaninkacebus* is the oldest known stem platyrrhine remains probable, but the limited morpho-paleontological data so far assembled (very few dental evidence and no cranial or post-cranial data) do not allow formalizing either hypothesis. This means that rooting (technically) the Platyrrhini in an Old World anthropoid clade in which either *Ashaninkacebus* or *Perupithecus* is nested requires further morphological support than current data allow.

Paleobiogeographic Implications. In addition to the Parapithecidae (19) and Oligopithecidae-like primates (12) of African origin, the eosimiid affinities of *Ashaninkacebus* point to a third clade of basal anthropoids involved in the Paleogene colonization of South America by primates. Eosimiids are well documented in the

Paleogene of South Asia (34, 46–50), but have not been formally recorded in the Eocene of Africa. However, our phylogenetic results resolved *Amamria* from the late middle Eocene of Tunisia [*ca.* 39.5 Ma (51)] nested within the Asian Eosimiidae clade (Fig. 2). *Amamria* is poorly documented (a single upper molar), but it represents, to date, the oldest known anthropoid primate in the fossil record of Africa. If it turns out that *Amamria* is indeed an eosimiid, this would support the hypothesis that this group of basal anthropoids of South Asian origin dispersed towards Africa, as was also the case for their closest relatives, the Afrotarsiidae (Fig. 2), and probably other basal anthropoids of Asian origin (35, 51–53). As surprising as it may seem, it is worth noting that while ancestral South Asian eosimiids dispersed across the Tethys Sea to invade Afro-Arabia sometime during the middle Eocene, they may also have continued their intercontinental dispersal across the Atlantic Ocean, and colonized South America in the process. Afro-Arabia could have been a mega-island stopover (biogeographic crossroad) between South Asia and South America for anthropoid primates and hystricognathous rodents (8, 51, 54).

Given the polyphyletic pattern of early anthropoids observed in the Paleogene sparse fossil record of Western Amazonia, questions remain as to whether there was a single rafting event or several ones (simultaneous or staggered in time) from Africa to South America. The paleobiogeographic issue becomes even more complicated when considering also hystricognathous rodents (“mass transit” or iterative rafting events). Although the time window during which the Afro-South American dispersal(s) occurred is now better bracketed, how and which routes primates and rodents might have taken to reach South America is a matter of speculation. However, habitat preferences and certain paleobiological attributes specific to these basal anthropoid primates and hystricognathous rodents may have increased their chances of both being unwillingly embarked on natural rafts (i.e., pieces of land and plants detached from the margins of large rivers during intense flooding events) and surviving during such an extraordinary over-water trip to South America from Africa (and from South Asia to Africa; ref. 53). Small-body sizes, insectivory/frugivory, arboreality (tree-dweller) in forested habitat near major river systems in Africa were likely key life-history traits that would have made these mammal groups especially prone to sweepstakes dispersal and survival on floating rafts, over larger-bodied, herbivorous animals living in forested or more open environments, away from riparian areas. Interestingly, our results of the BTD analysis suggest deep times for root age estimates, at least for the phylogenetic origins of *Ashaninkacebus* and *Perupithecus*, which can be traced back to the late middle Eocene (Fig. 2; an age range that is also estimated for the root of caviomorph rodents; ref. 16 and 26). The hyperthermal conditions of the late middle Eocene climatic optimum [MECO; ~40.5 Ma (55, 56)] resulted in particularly intense meteorological episodes in tropical/equatorial regions, most

certainly associated with intense flooding events (e.g., 57–59). These particular paleoenvironmental conditions may have enhanced riverbank break-ups more frequently, increasing the likelihood that some elements of riparian biological communities may have been carried away on natural rafts. Furthermore, the shorter distance between Africa and South America in the late middle Eocene might have increased the chances of successful transatlantic crossing(s) (6) rather than at a later time as advocated by Seiffert et al. (19), i.e., at or near the Eocene/Oligocene transition, during which a major drop in sea level is recorded, but when the two landmasses were actually much further apart. Trans-Tethyan dispersals of rodents and primates between South Asia and Africa (and/or other intervening landmasses) could also have been enhanced by the intense flooding events associated with the marked greenhouse climatic conditions of the MECO (35, 51–54, 60).

The presence of these small-bodied anthropoid primates in lower Oligocene deposits of Western Amazonia demonstrates the resilience of these lineages to the constraints of such a transatlantic dispersal, and their remarkable capacity to adapt, especially in foraging behaviors, in these new environments that became accessible to them. *Ashaninkacebus* and *Perupithecus* reveal that the ecological niche of these oldest known anthropoid primates from South America differed significantly from that of subsequent platyrrhines (33, 61–63). Formalizing more precisely the potential phylogenetic links of these early South American primates with the first known “true” platyrrhines would be a major achievement. This great challenge requires further paleontological data, especially substantial field efforts in tropical areas still severely under-sampled.

Materials and Methods

High-resolution μ -CT Scan. The three-dimensional (3D) data presented in this work were produced through the technical facilities of the *Instituto de Petróleo e dos Recursos Naturais, Pontifícia Universidade Católica do Rio Grande do Sul*, Brazil (high energy μ CT-scanning station SkyScan 1173). The unique UFAC-CS 066 fossil tooth was scanned with a resolution of 5.64 μ m. Avizo 2020.2 (Visualization Sciences Group) software was used for visualization, segmentation and 3D rendering. The 3D digital model of the tooth is available on the online open-access platform MorphoMuseuM (64).

Body Mass Estimation. Estimates of adult body mass (BM) were obtained using regression equations provided by Egi et al. (29) based on the M1 area (maximum mesiodistal length times maximum buccolingual breadth). It was calculated from 1) all primate sample equation: $\ln \text{ BM} = 1.713 \times \ln (\text{M1 area}) - 4.535$ (RE = 1.012); and 2) the anthropoid

equation: $\ln \text{BM} = 1.767 \times \ln (\text{M1 area}) - 4.555$ (RE = 0.950). The ratio estimator (RE) is the correction for logarithmic transformation bias (33, 65). The correction is applied by multiplying the predicted body mass by the RE.

Diet Reconstruction. An upper first molar shearing quotient (SQ) was calculated based on the sum of lengths of the buccal shearing crests 1 through 4 (66) with respect to the maximum mesiodistal tooth length (MDL). These lengths were measured on the 3D digital model of the UFAC-CS 066 M1 using Avizo 2020.2 measurement tools (“total shear” 1–4 = 2.84 mm; MDL = 2.03 mm). We followed the protocol of M1 SQ calculation and correction (using a Phylogenetic Generalized Least Squares [PGLS] model) provided and detailed in Kay et al. (33), modified from Allen et al. (67). We also used the platyrrhine dental measurement and diet dataset provided in Kay et al. (33).

Phylogenetic Reconstructions and Divergence-Time Estimation Between Taxa. The phylogenetic position of *Ashaninkacebus* in a high-level phylogeny including basal anthropoids (Old World, i.e., Paleogene South Asian and North African known taxa) and known extinct and extant platyrrhines was investigated (see [SI Appendix, Table S1](#)). We performed a cladistic assessment of the dental evidence (plus cranial and postcranial characters for several other taxa), as well as Bayesian tip-dating (BTD) analyses on the same morphological dataset to estimate divergence times between taxa (and also both, i.e., phylogeny and divergence times). A summary of the different types of analyses performed (A1 to A6) is provided in [SI Appendix, Table S2](#). We employed and updated the morphological matrix provided in Marivaux et al. (13), which itself was adapted and substantially modified from Kay (37). We incorporated in the matrix early anthropoid primates from the Paleogene of South Asia (i.e., Eosimiidae and Amphipithecidae) and North Africa (Parapithecidae, Oligopithecidae, and Propliopithecidae), as well as basal anthropoid taxa (*Amamria*, *Phileosimias*, *Afrasia*, and *Talahpithecus*), the phylogenetic status of some of which has not been formally established to date. The matrix also included primates recently discovered in South America (basal anthropoids and early platyrrhines), although some are poorly documented (*Perupithecus*, *Canaanimico*, *Panamacebus*, *Parvimico*, and *Ucayalipithecus*; [SI Appendix, Table S1](#)). All characters for all taxa in the total matrix were re-examined, and some upper and lower dentition characters were re-interpreted, adjusted or added to better describe the extent and variation of character states within basal and advanced anthropoids, and extinct and extant platyrrhines (see [SI Appendix, Dataset S1](#)). The final data matrix included 456 characters and 81 taxa (see [SI Appendix, Datasets S2 and S3](#)). We applied a molecular scaffold (68) on the datasets to recover those extant primate clades (Tarsiidae, Catarrhini, and Strepsirrhini) and notably Platyrrhini and within Platyrrhini clades that are strongly supported by genomic sequences.

The gene-based tree of extant taxa used as a constraint derives from several consistent molecular phylogenetic results (e.g., 21, 22, 69). Among Platyrrhini, this backbone tree enforces the monophyly of the three main families (and sub-families within): Cebidae (including Cebinae, Callitrichinae, and Aotinae), Atelidae (including Atelinae and Alouattinae), and Pitheciidae (including Callicebinae and Pitheciinae), the latter family being the most basal platyrrhine diverging clade. In our scaffold, Aotinae (*Aotus*) were considered as Cebidae *incertae sedis* since the competing hypotheses regarding their phylogenetic affinities either with cebines or callitrichines, or even with both (70, 71). The Pleistocene Caribbean primate taxon *Xenothrix* was also constrained as closely related to the callicebine pitheciid *Callicebus/Cheracebus* following recent ancient DNA analyses (38).

Parsimony Analyses. For the cladistic analyses (A1 and A2; [SI Appendix, Table S2](#)), additive multistate characters (i.e., conforming to natural morphoclines) were considered as ordered, and were scaled such that the sum of the steps equals 1 (13, 37). Characters were polarized via the out-group comparison method (72) using extinct and extant strepsirrhine primates (adapiforms and stem and crown strepsirrhines) and branching haplorrhine groups (tarsiiforms). The matrix for the parsimony analyses is provided in [SI Appendix, Dataset S2](#). The phylogenetic reconstructions were performed with PAUP 4.0a 169 (73) by heuristic searches (Hsearch) using random step-wise addition (1,000 replications with randomized input order of taxa) and tree-bisection-reconnection branch swapping options. Polymorphic *versus* uncertain character states (multistate taxa) were considered, and both were treated distinctly by PAUP (option *MSTaxa= Variable*). The clade robustness was measured by the Bremer Index (74) in equally weighted maximum-parsimony (after 1,000 iterations with randomized input order of taxa) (see [SI Appendix, Fig. S5](#)).

Bayesian Tip-Dating (BTD) Analyses. This Bayesian approach considers both the ages of the fossil taxa (tips) and rates of character evolution (75). For all the BTD analyses performed (A3 to A6; [SI Appendix, Table S2](#)), we selected the conditional version of the 1-parameter Markov-*k* model [Mkv (76)] for our total dataset, which includes only morphological data. The independent gamma rates (IGR) relaxed-clock model was applied to account for variation in morphological evolutionary rates among branches. The fossilized birth-death (FBD) process was used as a prior on branch lengths (in setting “*samplestrat*” to “*fossiltip*”), thus considering those tips left no descendant. Each fossil tip was calibrated with a uniform prior on age, corresponding to the minimum and maximum ages of each extinct taxon (i.e., stratigraphic range of a taxon, or upper and lower bounds of geological stages or Land Mammal Ages to which a fossil has been assigned, or even the error range of an absolute radiometric age; see [SI Appendix, Table S1](#)). Extant taxa were calibrated with a fixed prior on age set to present: *fixed(0)*. Regarding *Ashaninkacebus*, its stratigraphic context being

unknown (without considering the biochronological indication deriving from the associated rodent taxa from PRJ-33'), we have applied a very broad uniform temporal range prior on this taxon age, from the middle Eocene (45 Ma) to the late middle Miocene (13 Ma; the estimated age of the *in situ* PRJ-33 locality). The BTM analysis should return a median age estimate and a 95% highest posterior density (HPD) for *Ashaninkacebus* (e.g., 77). The FBD process was informed with a prior on the speciation rate ("*speciationpr*") set to *exp*(50), and flat beta priors (1.0, 1.0) associated with the fossilization rate and relative extinction rate ("*fossilizationpr*" and "*extinctionpr*", respectively). The tree root age was constrained to fall within a uniform prior from 56 Ma to 60 Ma, beyond which no representative of Euprimates has been recognized in the fossil record. For the gamma distribution from which the branch lengths are drawn ("*igrvarpr*"), this prior was set to *exp*(3). The prior on the rate of morphological changes, measured in the number of changes per character per millions of years ("*clockratepr*"), was set to *normal*(0.25, 0.05). The BTM analyses were performed with MrBayes 3.2.7a (78), using the computer cluster CIPRES Science Gateway 3.3 (79). As for the parsimony analyses, additive multistate characters were considered as ordered. Unlike PAUP, MrBayes treats all cases of polymorphism and uncertainty in the matrix as missing data (i.e., "?"), a drastic loss of morphological information that can seriously impact the phylogenetic reconstruction (see [SI Appendix, Text S2](#)). Given this, we first performed a BTM analysis by applying as hard constraints all nodes of the cladogram obtained with PAUP (A1), to estimate only the divergence times among taxa, not the phylogenetic relationships via a Bayesian approach (A3; Fig. 2; [SI Appendix, Fig. S7 and Text S3](#)). However, we also performed a partially constrained BTM analysis (A5) in enforcing only the molecular backbone tree of living species and the topology of the branching groups of Anthroidea plus outgroups, as resolved in A1 ([SI Appendix, Fig. S9 and Text S3](#)). BTM analyses were also conducted considering the Amphipithecidae as stem Anthroidea (A4 and A6; see [SI Appendix, Table S2, Figs. S8 and S10](#)). The different topological constraints for MrBayes (A3 to A6) were generated with R 4.2.1 (80), using the "ape" (81) and "paleotree" (82) R packages. The matrix and command lines for the BTM analyses and their variants are provided in [SI Appendix, Datasets S3 and S4](#). For each BTM analysis, two independent runs were performed simultaneously with four Monte Carlo Markov Chains (MCMC), with one cold and three heated (temp = 0.01) for 50 million generations per run. The MCMC were sampled every 1,000 generations, with a burn-in percentage of 25%. Convergence was assessed by checking the effective sample size (ESS) and the average standard deviation of split frequencies in the final generation (see [SI Appendix, Table S3](#)). For the A5 and A6 BTM analyses, an "allcompat" consensus tree was generated, summarizing all post-burn-in sampled trees. Several sensitivity analyses were performed with various perturbations of

the priors, notably “*igrvarpr*”, “*clockratepr*” and “*speciationpr*” (see [SI Appendix, Text S4](#)), which returned similar age estimates. Finally, using the RoguePlots approach (44), we assessed the uncertainty of the phylogenetic position of *Ashaninkacebus* across the posterior trees of the BTDA5 and A6 analyses after excluding the burn-in period.

Acknowledgments

We are very grateful to Adolpho Herbert Augustin (Institute of Petroleum and Natural Resources, Porto Alegre, Brazil) and Anne-Lise Charruault (ISE-M, France) for μ CT-scan acquisitions, treatments and reconstructions. We also thank Juliana Charão Marques and Daniel Triboli (LGI, *Universidade Federal do Rio Grande do Sul*, Porto Alegre, Brazil) for SEM microphotographs. We extend our gratitude to our Brazilian colleagues and students from the *Universidade Federal do Acre*, *Cruzeiro do Sul* and *Universidade de São Paulo*, who have contributed to some of the fieldwork seasons on the *Rio Juruá*. Special thanks go to the waterway staff (pirogues) and assistants for the logistics of the camps, as well as to the local people along the *Rio Juruá* for their hospitality and help in facilitating the fieldwork. We thank the Specialized Police Company of the 6th Military Police Unit of *Cruzeiro do Sul* (Acre), which ensured our security during the last field campaign on the *Rio Juruá* (August 2022). Chris Beard (guest Editor), as well as Erik Seiffert and two other anonymous reviewers provided formal reviews of this manuscript that enhanced the revised version. This research was supported by the *Brazilian Conselho Nacional de Desenvolvimento Científico e Tecnológico* (CNPq, 306951/2017-7, 312941/2018-8, 140773/2019-3, 310023/2021-1, and 310948/2021-5; CNPq/MCTI/CONFAP-FAPS PROTAX 22/2020 441626/2020-3, and FAPERGS 21/2551-0000781-8), *Coordenação de Aperfeiçoamento de Pessoal de Nível Superior* (CAPES, COFECUB program Te 924/18, 88881.143095/2017-01), the São Paulo Research Foundation (FAPESP, process 2011/14080-0 and 2019/14153-0), and the French *Agence Nationale de la Recherche* (ANR) in the framework of the LabEx CEBA (ANR-10-LABX-25-01; strategic project EMERGENCE).

References

1. R. Hoffstetter, R. Lavocat, Découverte dans le Déséadien de Bolivie de genres pentalophodontes appuyant les affinités des rongeurs caviomorphes. *C. R. Acad. Sci.* **271**, 172–175 (1970).
2. R. L. Ciochon, A. B. Chiarelli, “Paleobiogeographic perspectives on the origin of Platyrrhini” in *Evolutionary Biology of the New World Monkeys and Continental Drift*, R. L. Ciochon, A. B. Chiarelli, Eds. (Plenum Press, 1980), pp. 459–493.

3. A. Houle, The origin of platyrrhines: an evaluation of the Antarctic scenario and the floating island model. *Am. J. Phys. Anthropol.* **109**, 541–559 (1999).
4. J. G. Fleagle, C. C. Gilbert, “The biogeography of primate evolution: the role of plate tectonics, climate and chance” in *Primate Biogeography. Progress and Prospects*, S. M. Lehman, J. G. Fleagle, Eds. (Springer, 2006), pp. 375–418.
5. C. Poux, P. Chevret, D. Huchon, W. W. De Jong, E. J.-P. Douzery, Arrival and diversification of caviomorph rodents and platyrrhine primates in South America. *Syst. Biol.* **55**, 228–244 (2006).
6. F. Bandoni de Oliveira, E. C. Molina, G. Marroig, “Paleogeography of the South Atlantic: a route for primates and rodents into the New World?” in *South American Primates: Comparative Perspectives in the Study of Behavior, Ecology, and Conservation. Developments in Primatology. Progress and Prospects*, P. A. Garber, A. Estrada, J. C. Bicca-Marques, E. W. Heymann, K. B. Strier, Eds. (Springer+Business Media, 2009), pp. 55–68.
7. P. Perelman *et al.*, A molecular phylogeny of living Primates. *PLoS Genetics* **7**, e1001342 (2011).
8. P.-O. Antoine *et al.*, Middle Eocene rodents from Peruvian Amazonia reveal the pattern and timing of caviomorph origins and biogeography. *Proc. Royal Soc. B* **279**, 1319–1326 (2012).
9. C. G. Schrago, A. N. Menezes, C. Furtado, C. R. Bonvicino, H. N. Seuànez, Multispecies coalescent analysis of the early diversification of Neotropical primates: phylogenetic inference under strong gene trees/species tree conflict. *Gen. Biol. Evol.* **6**, 3105–3114 (2014).
10. N. S. Upham, B. D. Patterson, “Evolution of caviomorph rodents: a complete phylogeny and timetree for living genera” in *Biology of Caviomorph Rodents: Diversity and Evolution*, A. I. Vassallo, D. Antenucci, Eds. (SAREM Series A, 2015), pp. 63–120.
11. C. D. Frailey, K. E. Campbell, “Paleogene rodents from Amazonian Peru: the Santa Rosa local fauna” in *The Paleogene Mammalian Fauna of Santa Rosa, Amazonian Peru*, K. E. Campbell, Ed. (Natural History Museum of Los Angeles County, 2004), pp. 71–130.
12. M. Bond *et al.*, Eocene primates of South America and the African origins of New World monkeys. *Nature* **520**, 538–541 (2015).
13. L. Marivaux *et al.*, Neotropics provide insights into the emergence of New World monkeys: new dental evidence from the late Oligocene of Peruvian Amazonia. *J. Hum. Evol.* **97**, 159–175 (2016).
14. M. Boivin *et al.*, Late middle Eocene caviomorph rodents from Contamana, Peruvian Amazonia. *Palaeontol. Electron.* **50**, 1–50 (2017).
15. M. Boivin *et al.*, Early Oligocene caviomorph rodents from Shapaja, Peruvian Amazonia. *Palaeontographica Abt. A* **311**, 87–156 (2018).
16. M. Boivin, L. Marivaux, P.-O. Antoine, New insight from the Paleogene record of Amazonia into the early diversification of Caviomorpha (Hystricognathi, Rodentia): phylogenetic, macroevolutionary and paleobiogeographic implications. *Geodiversitas* **41**, 143–245 (2019).
17. M. Boivin *et al.*, Eocene caviomorph rodents from Balsayacu (Peruvian Amazonia). *Paläontol. Zeitsch.* **96**, 135–160 (2022).
18. M. Arnal, A. G. Kramarz, M. G. Vucetich, C. D. Frailey, K. E. Campbell, New Palaeogene caviomorphs (Rodentia, Hystricognathi) from Santa Rosa, Peru: systematics, biochronology, biogeography and early evolutionary trends. *Pap. Palaeontol.* **6**, 193–216 (2020).
19. E. R. Seiffert *et al.*, A parapathecoid stem anthropoid of African origin in the Paleogene of South America. *Science* **368**, 194–197 (2020).
20. M. Arnal, M. E. Pérez, L. M. Tejada Medina, K. E. Campbell, The high taxonomic diversity of the Palaeogene hystricognath rodents (Caviomorpha) from Santa Rosa (Peru, South America) framed within a new geochronological context. *Hist. Biol.*, early view (2022).
21. M. S. Springer *et al.*, Macroevolutionary dynamics and historical biogeography of primate diversification inferred from a species supermatrix. *PLoS ONE* **7**, e49521 (2012).
22. N. S. Upham, J. A. Esselstyn, W. Jetz, Inferring the mammal tree: species-level sets of phylogenies for questions in ecology, evolution, and conservation. *PLoS Biol.* **17**, e3000494. (2019).
23. A. H. Walton, “24. Rodents” in *Vertebrate Paleontology in the Neotropics. The Miocene Fauna of La Venta, Colombia*, R. F. Kay, R. H. Madden, R. L. Cifelli, J. J. Flynn, Eds. (Smithsonian Institution Press, 1997), pp. 392–409.

24. M. Boivin *et al.*, Late middle Miocene caviomorph rodents from Tarapoto, Peruvian Amazonia. *PLoS ONE* **16**, e0258455 (1-80) (2021).
25. L. Kerber *et al.*, Tropical fossil caviomorph rodents from the southwestern Brazilian Amazonia in the context of the South American faunas: systematics, biochronology, and paleobiogeography. *J. Mammal. Evol.* **24**, 57–70 (2017).
26. K. E. Campbell Jr, P. B. O’Sullivan, J. G. Fleagle, D. De Vries, E. R. Seiffert, An Early Oligocene age for the oldest known monkeys and rodents of South America. *Proc. Natl. Acad. Sci. U.S.A.* **118**, e2105956118 (2021).
27. P.-O. Antoine *et al.*, “Biotic community and landscape changes around the Eocene–Oligocene transition at Shapaja, Peruvian Amazonia: regional or global drivers?” in *Exploring the Impact of Andean Uplift and Climate on Life Evolution and Landscape Modification: From Amazonia to Patagonia*, C. Hoorn, L. Palazzesi, D. Silvestro, Eds. (Global and Planetary Change, 2021), p. Special Issue 103512.
28. P.-O. Antoine *et al.*, A 60-million-year Cenozoic history of western Amazonian ecosystems in Contamana, eastern Peru. *Gondwana Res.* **31**, 30–59 (2016).
29. N. Egi, M. Takai, N. Shigehara, T. Tsubamoto, Body mass estimates for Eocene eosimiid and amphipithecoid primates using prosimian and anthropoid scaling models. *Int. J. Primatol.* **25**, 211–236 (2004).
30. D. Silvestro *et al.*, Early arrival and climatically-linked geographic expansion of New World Monkeys from tiny African ancestors. *Syst. Biol.* **68**, 78–92 (2018).
31. Ford, S. M., Evolution of sexual dimorphism in body weight in platyrrhines. *Am. J. Primatol.* **34**, 221–244 (1994).
32. R. J. Smith, W. L. Jungers, Body mass in comparative primatology. *J. Hum. Evol.* **32**, 523–559 (1997).
33. R. F. Kay *et al.*, *Parvimico materdei* gen. et sp. nov.: a new platyrrhine from the Early Miocene of the Amazon Basin, Peru. *J. Hum. Evol.* **134**, 102628 (2019).
34. K. C. Beard, J. Wang, The eosimiid primates (Anthropoidea) of the Heti Formation, Yuanqu Basin, Shanxi and Henan Provinces, People’s Republic of China. *J. Hum. Evol.* **46**, 401–432 (2004).
35. Y. Chaimanee *et al.*, A new middle Eocene primate from Myanmar and the initial anthropoid colonization of Africa. *Proc. Natl. Acad. Sci. U.S.A.* **109**, 10293–10297 (2012).
36. R. F. Kay, J. G. Fleagle, Stem taxa, homoplasy, long lineages, and the phylogenetic position of *Dolichocebus*. *J. Hum. Evol.* **59**, 218–222 (2010).
37. R. F. Kay, Biogeography in deep time - What do phylogenetics, geology, and paleoclimate tell us about early platyrrhine evolution? *Mol. Phylogenet. Evol.* **82**, 358–374 (2015).
38. R. Woods, S. T. Turvey, S. Brace, R. D. E. MacPhee, I. Barnes, Ancient DNA of the extinct Jamaican monkey *Xenothrix* reveals extreme insular change within a morphologically conservative radiation. *Proc. Natl. Acad. Sci. U.S.A.* **115**, 12769–12774 (2018).
39. M. Rivero, O. Arredondo, *Paralouatta varonai*, a new Quaternary platyrrhine from Cuba. *J. Hum. Evol.* **21**, 1–11 (1991).
40. J.-J. Jaeger *et al.*, Amphipithecine primates are stem anthropoids: cranial and postcranial evidence. *Proc. Roy. Soc. B* **287**, 20202129 (2020).
41. J. E. O’Reilly, M. Dos Reis, P. C. J. Donoghue, Dating tips for divergence-time estimation. *Trends Genet.* **31**, 637–650 (2015).
42. R. M. D. Beck, M. S. Y. Lee, Ancient dates or accelerated rates? Morphological clocks and the antiquity of placental mammals. *Proc. Royal Soc. B* **281**, 20141278 (2014).
43. R. M. D. Beck, D. De Vries, M. C. Janiak, I. B. Goodhead, J. P. Boubli, Total evidence phylogeny of platyrrhine primates and a comparison of undated and tip-dating approaches. *J. Hum. Evol.* **174**, 103293 (2023).
44. S. Klopstein, T. Spasojevic, Illustrating phylogenetic placement of fossils using RoguePlots: An example from ichneumonid parasitoid wasps (Hymenoptera, Ichneumonidae) and an extensive morphological matrix. *PLoS ONE* **14**, e0212942 (2019).
45. E. C. Kirk, E. L. Simons, Diets of fossil primates from the Fayum Depression of Egypt: a quantitative analysis of molar shearing. *J. Hum. Evol.* **40**, 203–229 (2001).
46. K. C. Beard, T. Qi, M. R. Dawson, B. Wang, C. Li, A diverse new primate fauna from middle Eocene fissure-fillings in southeastern China. *Nature* **368**, 604–609 (1994).

47. K. C. Beard, Y. Tong, M. R. Dawson, J. Wang, X. Huang, Earliest complete dentition of an anthropoid primate from the late middle Eocene of Shanxi Province, China. *Science* **272**, 82–85 (1996).
48. J.-J. Jaeger *et al.*, A new primate from the middle Eocene of Myanmar and the Asian early origin of anthropoids. *Science* **286**, 528–530 (1999).
49. L. Marivaux *et al.*, Anthropoid primates from the Oligocene of Pakistan (Bugti Hills): data on early anthropoid evolution and biogeography. *Proc. Natl. Acad. Sci. U.S.A.* **102**, 8436–8441 (2005).
50. X. Ni, Q. Li, L. Li, K. C. Beard, Oligocene primates from China reveal divergence between African and Asian primate evolution. *Science* **352**, 673–677 (2016).
51. L. Marivaux *et al.*, A morphological intermediate between eosimiiform and simiiform primates from the late middle Eocene of Tunisia: macroevolutionary and paleobiogeographic implications of early anthropoids. *Am. J. Phys. Anthropol.* **154**, 387–401 (2014).
52. J.-J. Jaeger *et al.*, Late middle Eocene epoch of Libya yields earliest known radiation of African anthropoids. *Nature* **467**, 1095–1098 (2010).
53. K. C. Beard, Out of Asia: anthropoid origins and the colonization of Africa. *Ann. Rev. Anthropol.* **45**, 199–213 (2016).
54. L. Marivaux, M. Boivin, Emergence of hystricognathous rodents (Mammalia, Hystricognathi): Palaeogene fossil record, phylogeny, macroevolution and historical biogeography. *Zool. J. Linn. Soc.* **187**, 929–964 (2019).
55. S. M. Bohaty, J. C. Zachos, F. Florondo, M. L. Delaney, Coupled greenhouse warming and deep-sea acidification in the middle Eocene. *Paleoceanography* **24**, PA2207 (2009).
56. R. P. Speijer, H. Pälike, C. J. Hollis, J. J. Hooker, J. G. Ogg, The Paleogene period. *Geological Time Scale 2020* **2**, 1087–1140 (2020).
57. A. Mulch *et al.*, Rapid change in high-elevation precipitation patterns of Western North America during the Middle Eocene Climatic Optimum (MECO). *Am. J. Sci.* **315**, 317–336 (2015).
58. R. D’Onofrio *et al.*, Impact of the Middle Eocene Climatic Optimum (MECO) on foraminiferal and calcareous nannofossil assemblages in the Neo-Tethyan Baskil section (eastern Turkey): paleoenvironmental and paleoclimatic reconstructions. *Appl. Sci.* **11**, 11339 (2021).
59. S. Peris Cabré *et al.*, Fluvio-deltaic record of increased sediment transport during the Middle Eocene Climatic Optimum (MECO), Southern Pyrenees, Spain. *EGUsphere*, in press (2022).
60. K. C. Beard, G. Métails, F. Ocakoğlu, A. Licht, An omomyid primate from the Pontide microcontinent of north-central Anatolia: Implications for sweepstakes dispersal of terrestrial mammals during the Eocene. *Geobios* **66–67**, 143–152 (2021).
61. R. F. Kay, “A new primate from the early Miocene of Gran Barranca, Chubut Province, Argentina: paleoecological implications” in *The Paleontology of Gran Barranca: Evolution and Environmental Change through the Middle Cenozoic of Patagonia*, R. H. Madden, A. A. Carlini, M. G. Vucetich, R. F. Kay, Eds. (Cambridge University Press, 2010), pp. 216–235.
62. R. F. Kay, New World monkey origins. Fossils in Peru raise questions about the early evolution of monkeys in South America. *Science* **347**, 1068–1069 (2015).
63. R. F. Kay *et al.*, “Paleobiology of Santacrucian primates” in *Early Miocene Paleobiology in Patagonia: High-Latitude Paleocommunities of the Santa Cruz Formation*, S. F. Vizcaino, R. F. Kay, M. S. Bargo, Eds. (Cambridge University Press, 2012), pp. 306–330.
64. L. Marivaux, F. R. Negri, A. M. Ribeiro, 3D model related to the publication: An eosimiid primate of South Asian affinities in the Paleogene of Western Amazonia and the origin of New World monkeys. *MorphoMuseum*, e188, in press (2023). <https://doi.org/10.18563/journal.m3.188>
65. R. J. Smith, Logarithmic transformation bias in allometry. *Am. J. Phys. Anthropol.* **90**, 215–228 (1993).
66. R. F. Kay, The evolution of molar occlusion in the Cercopithecidae and early catarrhines. *Am. J. Phys. Anthropol.* **46**, 327–352 (1977).
67. K. L. Allen, S. B. Cooke, L. A. Gonzales, R. F. Kay, Dietary inference from upper and lower molar morphology in platyrrhine primates. *PLoS ONE* **10**, e0118732 (2015).
68. M. S. Springer, E. Teeling, O. Madsen, M. J. Stanhope, W. W. De Jong, Integrated fossil and molecular data reconstruct bat echolocation. *Proc. Natl. Acad. Sci. U.S.A.* **98**, 6241–6246 (2001).

69. N. M. Jameson Kiesling, S. V. Yi, K. Xu, F. G. Sperone, D. E. Wildman, The tempo and mode of New World monkey evolution and biogeography in the context of phylogenomic analysis. *Mol. Phylogenet. Evol.* **82**, 386–399 (2015).
70. H. Schneider, I. Sampaio, The systematics and evolution of New World primates – A review. *Mol. Phylogenet. Evol.* **82**, 348–357 (2015).
71. C. G. Schrago, H. N. Seuánez, Large ancestral effective population size explains the difficult phylogenetic placement of owl monkeys. *Am. J. Primatol.* **81**, e22955 (2019).
72. L. E. Watrous, Q. D. Wheeler, The outgroup comparison method of character analysis. *Syst. Zool.* **30**, 1–11 (1981).
73. D. L. Swofford, PAUP*. Phylogenetic Analysis Using Parsimony (*and Other Methods). Version 4. (2002).
74. K. Bremer, The limits of amino acid sequence data in angiosperm phylogenetic reconstruction. *Evolution* **42**, 795–803 (1988).
75. F. Ronquist *et al.*, A total-evidence approach to dating with fossils, applied to the early radiation of the Hymenoptera. *Syst. Biol.* **61**, 973–999 (2012).
76. P. O. Lewis, A Likelihood approach to estimating phylogeny from discrete morphological character data. *Syst. Biol.* **50**, 913–925 (2001).
77. J. Barido-Sottani, D. Żyła, T. A. Heath, Estimating the age of poorly dated fossil specimens and deposits using total-evidence approach and the fossilized birth-death process. *Syst. Biol.*, in press (2023).
78. F. Ronquist *et al.*, MrBayes 3.2: efficient Bayesian phylogenetic inference and model choice across a large model space. *Syst. Biol.* **61**, 539–542 (2012).
79. M. A. Miller *et al.*, A RESTful API for access to phylogenetic tools via the CIPRES Science Gateway. *Evol. Bioinf.* **11**, 43–48 (2015).
80. R Development Core Team, *R: A Language and Environment for Statistical Computing* (Foundation for Statistical Computing, 2018).
81. E. Paradis, K. Schliep, ape 5.0: an environment for modern phylogenetics and evolutionary analyses in R. *Bioinformatics* **35**, 526–528 (2019).
82. D. W. Bapst, paleotree: an R package for paleontological and phylogenetic analyses of evolution. *Methods Ecol. Evol.* **3**, 803–807 (2012).

Figures and Tables

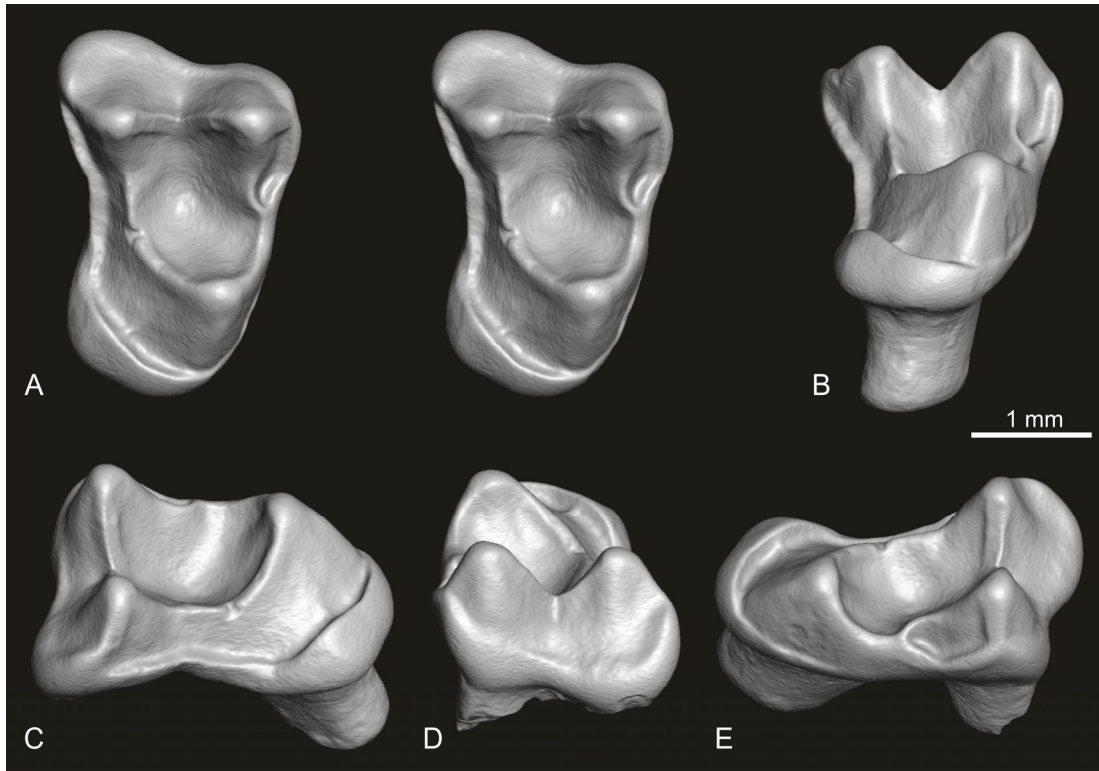


Figure 1. Right first upper molar of *Ashaninkacebus simpsoni* gen. et sp. nov. (UFAC-CS 066, holotype) from PRJ-33' locality, *Rio Juruá (Alto Yuruá)*, State of Acre, Brazil. Buccolingual width: 2.92 mm; mesiodistal length: 2.03 mm. (A) Stereopair in occlusal view; (B) lingual view; (C) distal view; (D) buccal view; (E) mesial view. Images are renderings of a 3D digital model of the fossil specimen, obtained by X-ray micro-computed (μ CT) surface reconstruction (segmented enamel surface).

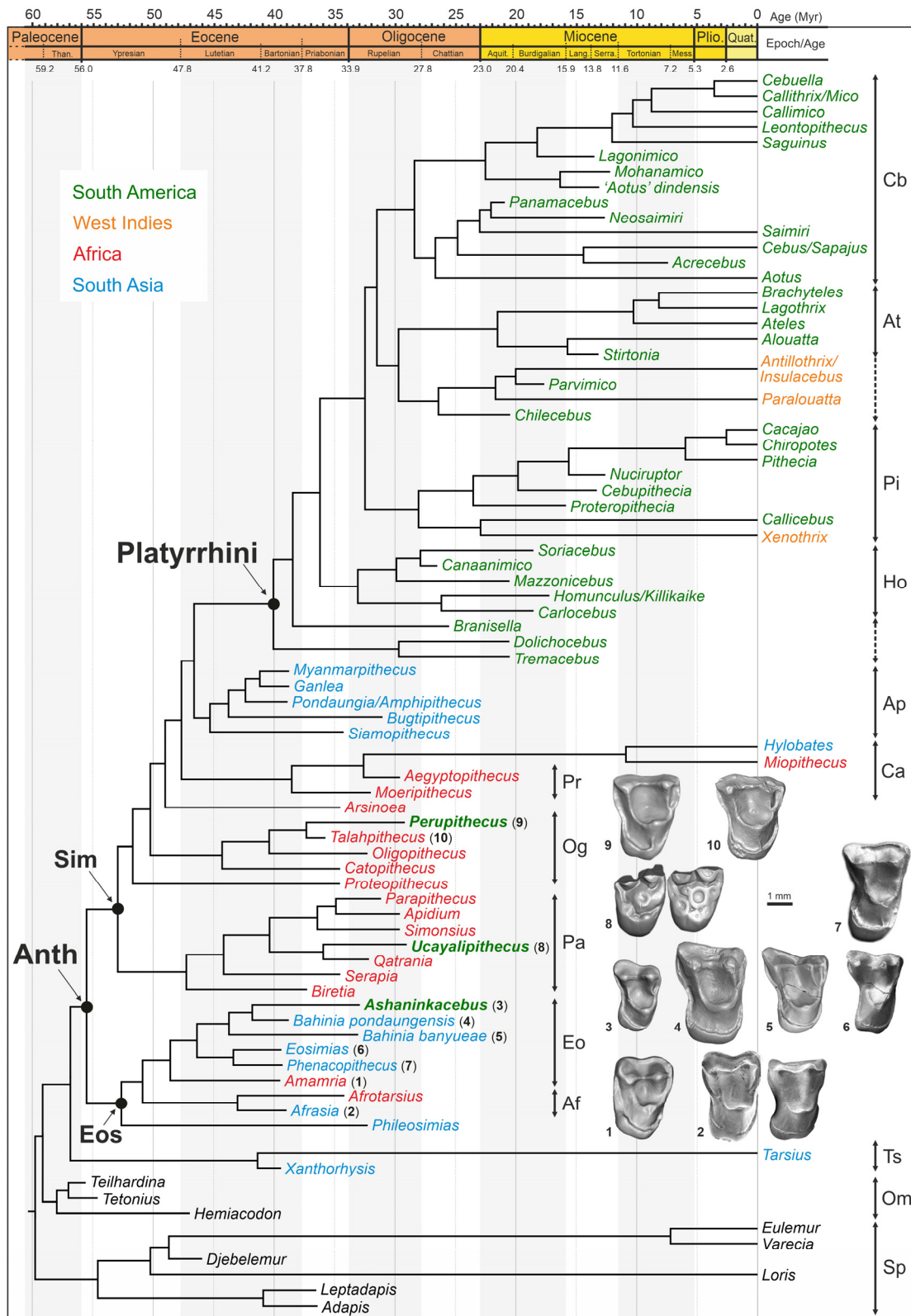


Figure 2. Phylogenetic position of *Ashaninkacebus simpsoni* gen. et sp. nov. in a high-level phylogeny of basal anthropoids (Old World, i.e., Paleogene South Asian and North African known taxa), plus known extinct and extant platyrrhines, deriving from a cladistic assessment of the craniodental and postcranial evidence. Single most-parsimonious tree of 2429.49 steps (Consistency index [CI] = 0.36; Retention index [RI] = 0.56), which was obtained after analyses performed in considering some ordered and scaled multistate characters, and in applying a molecular scaffold of living taxa relationships (See Methods). The cladogram was then subjected to a Bayesian tip-dating analysis (BTD) for divergence-time estimation between taxa. Abbreviations: **Af**, Afrotarsiidae; **Anth**, Anthropeidea; **Ap**, Amphipithecidae; **At**, Atelidae; **Ca**, Catarrhini; **Cb**, Cebidae; **Eo**, Eosimiidae; **Eos**, Eosimiiformes; **Ho**, Homunculidae; **Og**, Oligopithecidae; **Om**, Omomyiformes; **Pa**, Parapithecidae; **Pi**, Pitheciidae; **Pr**, Propithecidae; **Sim**, Simiiformes; **Sp**, strepsirrhines; **Ts**, Tarsiidae. Upper molars of some basal anthropoids for comparisons: **1**, KEB-1-001 right M2 of *Amamria tunisiensis* (ref. 51, their figure 3A); **2**, NMMP-85 right M1 and NMMP-81 M2 of *Afrasia djijidae* (ref. 35, their figure 2A–B); **3**, UFAC-CS 066 right M1 of *Ashaninkacebus simpsoni* gen. et sp. nov. (this paper); **4**, M1 of the NMMP-15 right maxillary of *Bahinia pondaungensis* (ref. 48; here 3D rendering of a cast scan); **5**, IVPP V22730 right M1 of *Bahinia banyueae* (ref. 50, their figure 1F); **6**, IVPP V11993 left M1 (reversed) of *Eosimias centennicus* (ref. 34, their figure 9); **7**, IVPP V11997 right M2 of *Phenacopithecus krishtalkai* (ref. 34, their figure 22); **8**, CPI-7937 right M1 and CPI-7938 left M2 (reversed) of *Ucayalipithecus perdita* (ref. 19, their figure 1A); **9**, CPI-6486 right M1 of *Perupithecus ucayaliensis* (ref. 12, 19, their figure 1D); **10**, DT1-31 left M1 (reversed) of *Talahpithecus parvus* (ref. 52, their figure 2N; here 3D rendering of a cast scan).

Supporting Information for

An eosimiid primate of South Asian affinities in the Paleogene of Western Amazonia and the origin of New World monkeys

Laurent Marivaux*, Francisco R. Negri, Pierre-Olivier Antoine, Narla S. Stutz, Fabien L. Condamine, Leonardo Kerber, François Pujos, Roberto Ventura Santos, André M. V. Alvim, Annie S. Hsiou, Marcos C. Bissaro Júnior, Karen Adami-Rodrigues, and Ana Maria Ribeiro

*Corresponding author: Laurent Marivaux

Email: Laurent.Marivaux@UMontpellier.fr

This PDF file includes:

Figures S1 to S12
Texts S1 to S4
Tables S1 to S4
SI References

Other supporting materials for this manuscript include the following:

Datasets S1 to S4



Fig. S1. Geographic location of the Foz do Breu area, State of Acre, Brazil (Western Brazilian Amazonia) and of the vertebrate PRJ-33 fossil-bearing locality ($9^{\circ}24'24.6''\text{S}$ $72^{\circ}43'27.6''\text{W}$), nearby which allochthonous Holocene detrital sediments (PRJ-33', transported blocks of microconglomerate) have yielded the isolated tooth of *Ashaninkacebus simpsoni* gen. et sp. nov. PRJ-33 and PRJ-33' are exposed on the left bank of the *Rio Juruá* (*Alto Yurúa*), 1 km upstream from the junction with the *Rio Breu* and the small village of *Foz do Breu*. The PRJ-33' sediments are deposited directly beneath the *in situ* PRJ-33 fossil-bearing locality. The black star indicates the fossil-bearing locality of Santa Rosa in Peru (situated on the *Alto Yurúa*, 22 km upstream of PRJ-33 in Brazil). Abbreviations: **EC.**, Ecuador; **FG.**, French Guiana; **G.**, Guiana; **N**, North; **PA.**, Paraguay; **PRJ**, *Ponto Rio Juruá*; **SU.**, Surinam; **UR.**, Uruguay.

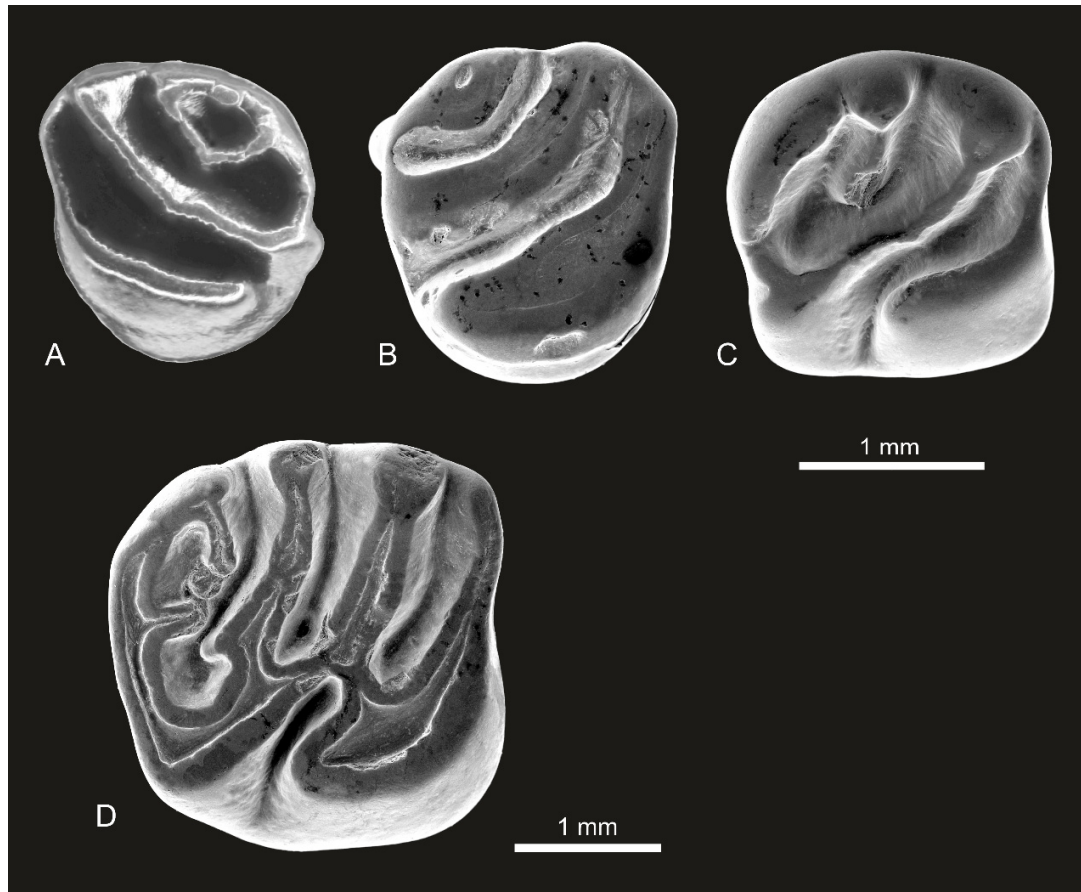


Fig. S2. Scanning electron microscope photographs of the isolated teeth of caviomorph rodents found in the same PRJ-33' allochthonous primate-yielding sediments. (A–C) *Eoimcamys* sp. [*E. pascuali* sensu Ribeiro et al. (ref. 1) or Arnal et al. (ref. 2)]: (A) UFAC-CS 016, left upper M2 or M3 (ref. 1, their figure 2); (B) UFAC6-CS 018, worn right upper M2 or M3; (C) UFAC-CS 053, right upper M1. (D) *Cachiyacuy* sp.: UFAC-CS 215, right upper M1. Teeth are shown in occlusal views.

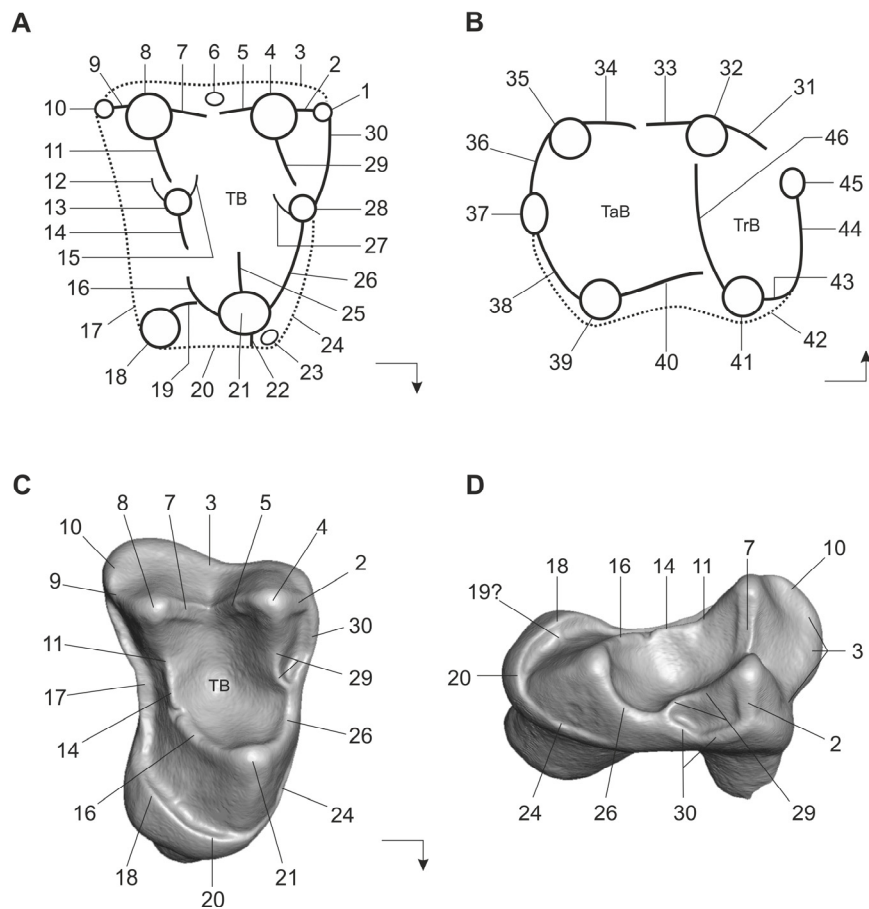


Fig. S3. Dental nomenclature. (A–B) Schematic occlusal dental morphology of upper (A) and lower (B) teeth of primates and related nomenclature (used for the selected characters of the phylogenetic analyses). The dental terminology is after Marivaux et al. (3), modified after Szalay and Delson (4) and Marivaux (5). (C–D) 3D digital model of the UFAC-CS 066 holotype (right upper M1) of *Ashaninkacebus simpsoni* gen. et sp. nov. (described in this article) and related nomenclature in occlusal (C) and mesial (D) views of the dental specimen. The images have been obtained by X-ray μ CT surface reconstruction. The arrows situated in front of the molars indicate the orientation of the teeth on the jaws (mesiolingual).

Upper molars: 1, parastyle; 2, preparacrista; 3, buccal cingulum; 4, paracone; 5, postparacrista; 6, mesostyle; 7, premetacrista; 8, metacone; 9, postmetacrista; 10, metastyle (or metastylar shelf); 11, hypometacrista; 12, postmetaconule crista; 13, metaconule; 14, hypometaconule crista (= metacrista or crista obliqua); 15, premetaconule crista; 16, postprotocrista; 17, distal cingulum; 18, hypocone; 19, prehypocrista; 20, lingual cingulum; 21, protocone; 22, entoprotocrista; 23, pericone; 24, mesial cingulum; 25, endoprotocrista; 26, preprotocrista; 27, postparaconule crista; 28, paraconule; 29, hypoparacrista; 30, preparaconule crista; TB, trigon basin; 2 + 5 + 7 + 9, eocrista; 11 + 14, hypometacrista/metacrista complex (or hypometacrista complex).

Lower molars: 31, premetacristid; 32, metaconid; 33, postmetacristid; 34, pre-entocristid; 35, entoconid; 36, postentocristid; 37, hypoconulid; 38, hypocristid; 39, hypoconid; 40, cristid obliqua; 41, protoconid; 42, buccal cingulid; 43, buccal paracristid; 44, mediolingual paracristid; 45, paraconid; 46, protocristid; TaB, talonid basin; TrB, trigonid basin.

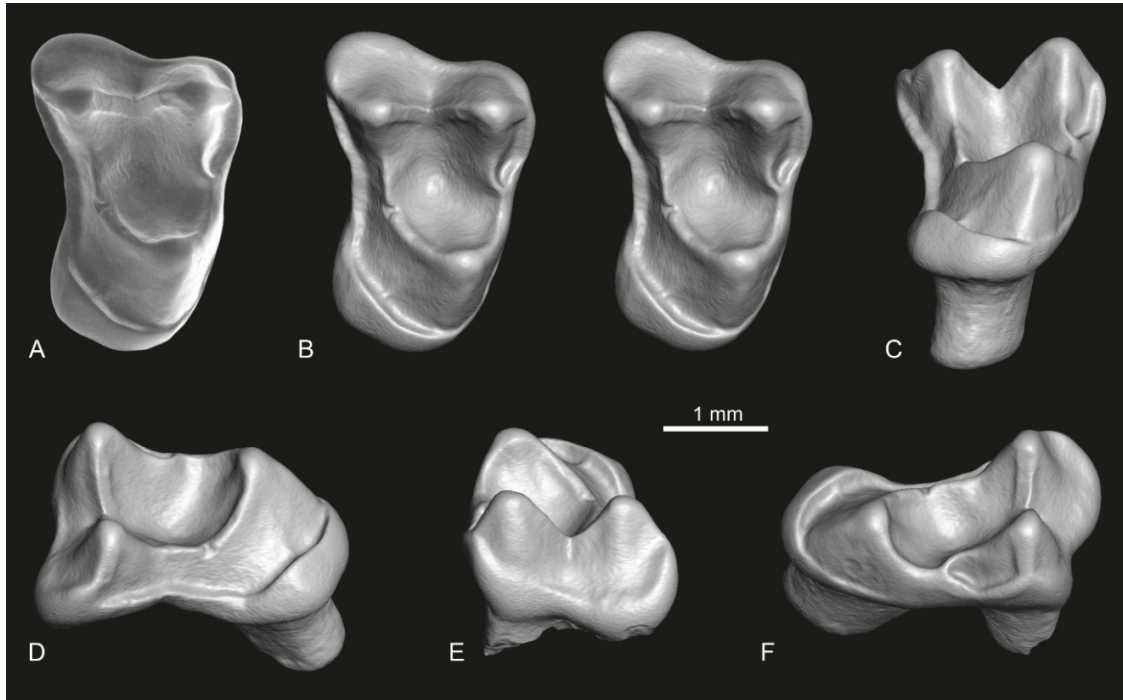


Fig. S4. UFAC-CS 066 (holotype), right first upper molar (M1) of *Ashaninkacebus simpsoni* gen. et sp. nov. (A) Scanning electron microscope photograph of the fossil specimen in occlusal view; (B–F) Image renderings of the segmented enamel surface of the fossil specimen in occlusal (B; stereopair), lingual (C), distal (D), buccal (E), and mesial (F) views. The 3D digital model of the fossil dental specimen was obtained by X-ray micro-computed (μ CT) surface reconstruction.

Text S1. Description of the UFAC-CS 066 dental specimen.

UFAC-CS 066 is a complete and pristine right M1 (Fig. S4). It is three-rooted, but only a portion of the lingual root is preserved, the two buccal roots are broken at the cervix. There is neither mesial nor distal trace of contact facets, and the main occlusal structures (cups and crests) do not show attritional wear, thereby indicating that this tooth had not yet erupted (i.e., belonged to a young individual). The tooth is low crowned and much broader transversely than it is long (buccolingual width: 2.92 mm; mesiodistal length: 2.03 mm). It is primarily tritubercular with acute protocone, paracone and metacone, associated with a set of low but trenchant longitudinal and transverse crests, and well-marked lingual, distal and buccal cingula. Metaconule and paraconule are absent, or at least indistinguishable from the structures that connect them. The lingual cingulum is mesiodistally complete, but stronger in the distal region than in the mesial region. Distally, it bears a small swelling of enamel, stretched mesiodistally, which marks the presence of a minute hypocone. The latter lies slightly more lingual than the protocone. A deep sulcus separates both lingual cusps. However, a very short and very low enamel crestule, faintly visible, occurs in the sulcus between the protocone and the minute hypocone. Directly lingual to the protocone, the cingulum is faintly developed, thin and in continuity with an equally thin and short mesial cingulum, which ends in merging with the base of the crown, at a point mesiobuccal to the protocone. In contrast, the distal cingulum is particularly well defined, forming a low, narrow and concave full-fledged shelf of enamel, extending from the cingular hypocone to the buccal base of the crown, at a point distobuccal to the metacone. The deep concavity of the distal cingulum and the weak development of the hypocone make the distal crown margin markedly invaginated (waisted). The protocone is mesially canted and aligned almost buccolingually with the paracone. These two mesial cusps are roughly equal in size. The metacone is slightly smaller, and lies distal to the paracone, being closer to the paracone than the latter is to the protocone. The mesiodistal alignment of the paracone with the metacone, and the marked distal waisting of the crown are features that allow this tooth to be identified as a M1 rather than a M2. Buccally, the flanks of the paracone and metacone are not strongly convex (not buccally extensive), appearing somewhat moderately steep-sided. A complete and continuous buccal cingulum is clearly visible at the base of both cusps. This cingulum is relatively discrete at the base of the paracone, whereas it is particularly well developed and buccally extensive at the level of the metacone, giving this cusp an internal position on the buccal margin. The distobuccal cingulum forms a rounded lobe-like structure, which incorporates a minute and cristiform metastyle (i.e., curved metastylar shelf) occupying a buccal position relative to the metacone. The metastylar shelf is linked to the metacone by a moderately long and slightly arcuate postmetacrista. In contrast, the premeta-, postpara- and prepara- cristae are aligned mesiodistally. The latter are well developed, particularly sharp and gently-sloping, forming with the postmetacrista, a W-shaped shearing eocrista (in buccal perspective). Mesiobuccally, the preparacrista is shorter than the other buccal cristae, and there is no appreciable development of a parastyle in its mesial extremity. Lingually, the protocone displays well-defined, long and buccally oriented pre- and post-protocone cristae (U-shaped protocone cristae), which circumscribe a narrow trigon basin lingually. The preprotocrista extends mesiobuccally, steeply from the apex of the protocone up the location where a paraconule would normally occur (it is absent), then continues buccally beyond that point (via the preparaconule crista) to reach the mesial extremity of the preparacrista. A long, thin but well-marked hypoparacrista arises from the lingual flank of the paracone, extends lingually in a gentle slope, and turns sharply mesially at the midline of the tooth to connect to the preprotocrista. Distally and parallel to the hypoparacrista, a short but well-defined hypometacrista arises at mid-slope of the lingual flank of the metacone, and connects to an extremely small

enamel swelling that could correspond to a remnant of a metaconule. From this enamel swelling, a short crest (hypometaconule crista/metacrista) extends lingually towards the buccal extremity of the postprotocrista, but it does not reach it. A narrow but well-marked notch, situated near the midline of the tooth, separates the two crests.

Table S1. Selected primate taxa for the phylogenetic analyses (A1 to A6) with information regarding their provenance and age range.

Taxa	species observed	Epoch or Interval (temporal range)	LMA	Age or range (Myr)	TRP - BTD (Myr)	Provenance(s)	References (figured or refigured observed material, and age information)
<i>Cebuella</i>	<i>pygmaea</i>	Extant	-	-	Fixed(0)	Peru	Possible early Late Miocene (at least) occurrence of the genus; see Marivaux <i>et al.</i> (6)
<i>Callithrix / Mico</i>	<i>(M.) emiliae & (M.) argentata</i>	Extant	-	-	Fixed(0)	Brazil	-
<i>Saguinus</i>	<i>midas</i>	Extant	-	-	Fixed(0)	Brazil	-
<i>Leontopithecus</i>	<i>rosalia</i>	Extant	-	-	Fixed(0)	Brazil	-
<i>Lagonimico</i>	<i>conclucatus</i>	late middle Miocene	Laventan SALMA	13.6-13.4	Uniform(13.4,13.6)	Honda group, La Venta, Colombia	Kay (7)
<i>Mohanamico</i>	<i>hershkovitzi</i>	late middle Miocene	Laventan SALMA	12.2	Uniform(12,12.4)	Honda group, La Venta, Colombia	Luchterhand <i>et al.</i> (8)
<i>Callimico</i>	<i>goeldii</i>	Extant	-	-	Fixed(0)	Peru	-
<i>Cebus / Sapajus</i>	<i>(C.) capucinus & (S.) apella</i>	Extant	-	-	Fixed(0)	Panama & Brazil, respectively	Possible early Late Miocene (at least) occurrence of the genus; see Marivaux <i>et al.</i> (6)
<i>Acrecebus</i>	<i>fraileyi</i>	late late Miocene	Huayquerian SALMA	9-6	Uniform(6,9)	Bandeira, Acre, Brazil	Kay and Cozzuol (9)
<i>Panamacebus</i>	<i>transitus</i>	earliest Miocene	Arikareean NALMA	21.1-20.76	Uniform(20.76,21.1)	Lirio Norte, Las Cascadas Fm., Panama Canal	Bloch <i>et al.</i> (10)
<i>Saimiri</i>	<i>sciureus & oerstedii</i>	Extant	-	-	Fixed(0)	Brazil & Panama, respectively	-
<i>Neosaimiri</i>	<i>fieldsi</i>	late middle Miocene	Laventan SALMA	13.2-12	Uniform(12,13.2)	Honda group, La Venta, Colombia	Stirton (11); Takai (12); Nakatsukasa <i>et al.</i> (13)
<i>Aotus</i>	<i>trivirgatus</i>	Extant	-	-	Fixed(0)	Brazil	-
" <i>Aotus</i> "	<i>dindensis</i>	late middle Miocene	Laventan SALMA	13.2-13	Uniform(13,13.2)	Honda group, La Venta, Colombia	Setoguchi and Rosenberger (14)
<i>Callicebus</i>	<i>brunneus</i>	Extant	-	-	Fixed(0)	Brazil	-
<i>Pithecia</i>	<i>irrorata</i>	Extant	-	-	Fixed(0)	Brazil	-
<i>Cacajao</i>	<i>melanocephalus</i>	Extant	-	-	Fixed(0)	Brazil	-
<i>Chiropotes</i>	<i>satanas & albinasus</i>	Extant	-	-	Fixed(0)	Brazil	-
<i>Cebupithecia</i>	<i>sarmiento</i>	late middle Miocene	Laventan SALMA	13.6-13	Uniform(13.6,13)	Honda group, La Venta, Colombia	Stirton (11); Bloch <i>et al.</i> (10)
<i>Nuciraptor</i>	<i>rubricae</i>	late middle Miocene	Laventan SALMA	12.8-12.4	Uniform(12.8,12.4)	Honda group, La Venta, Colombia	Meldrum and Kay (15)
<i>Proteropithecia</i>	<i>neuquenensis</i>	early middle Miocene	Colloncuran SALMA	15.7	Uniform(16,15.7)	Cañadon del Tordillo, Neuquen Prov., Argentina	Kay <i>et al.</i> (16-17)
<i>Alouatta</i>	<i>belzebul & seniculus</i>	Extant	-	-	Fixed(0)	Brazil	-

Taxa	species observed	Epoch or Interval (temporal range)	LMA	Age or range (Myr)	TRP - BTD (Myr)	Provenance(s)	References (figured or refigured observed material, and age information)
<i>Ateles</i>	<i>geoffroyi</i>	Extant	-	-	Fixed(0)	Panama	-
<i>Brachyteles</i>	<i>arachnoides</i>	Extant	-	-	Fixed(0)	Brazil	-
<i>Lagothrix</i>	<i>lagotricha</i>	Extant	-	-	Fixed(0)	Brazil	-
<i>Stirtonia</i>	<i>tatacoensis</i>	late middle Miocene	Laventan SALMA	13.6-12.8	Uniform(12.8,13.6)	Honda group, La Venta, Colombia	Stirton (11); Hershkovitz (18); Setoguchi <i>et al.</i> (19); Bloch <i>et al.</i> (10)
<i>Chilecebus</i>	<i>carrascoensis</i>	earliest Miocene	Colhuehuapian SALMA	21-20	Uniform(20,21)	Abanico Fm., Chile	Flynn <i>et al.</i> (20)
<i>Mazzonicebus</i>	<i>almendrae</i>	earliest Miocene	Colhuehuapian SALMA	21-20	Uniform(20,21)	Gran Barranca, Chubut Prov., Argentina	Kay (21)
<i>Homunculus</i>	<i>patagonicus</i> & (" <i>Killikaike</i> ") <i>blakei</i>	late early Miocene	Santacrucian SALMA	17.9-16.5	Uniform(16.5,17.9)	Santa Cruz Fm., Santa Cruz Prov., Argentina	Ameghino (22–23); Bluntschli (24); Hershkovitz (25); Tejedor <i>et al.</i> (26); Perry <i>et al.</i> (27)
<i>Soriacebus</i>	<i>ameghinorum</i>	early Miocene	Santacrucian (" <i>Pinturan</i> ") SALMA	19-18	Uniform(18,19)	Pinturas Fm., Santa Cruz Prov., Argentina	Fleagle <i>et al.</i> (28); Fleagle (29)
<i>Carlocebus</i>	<i>intermedius</i> & <i>carmenensis</i>	early Miocene	Santacrucian (" <i>Pinturan</i> ") SALMA	19-18	Uniform(18,19)	Pinturas Fm., Santa Cruz Prov., Argentina	Fleagle (29); Anapol and Fleagle (30)
<i>Dolichocebus</i>	<i>gaimanensis</i>	earliest Miocene	Colhuehuapian SALMA	21-20	Uniform(20,21)	Gaiman, Chubut Prov., Argentina	Kraglievich (31); Fleagle and Bown (32); Reeser (33); Kay <i>et al.</i> (34)
<i>Tremacebus</i>	<i>harringtoni</i>	earliest Miocene	Colhuehuapian SALMA	21-20	Uniform(20,21)	Sacanana, Chubut Prov., Argentina	Hershkovitz (35)
<i>Canaanimico</i>	<i>amazonensis</i>	late Oligocene	Deseadan SALMA	26.5	Uniform(26.6,26.4)	CTA-61, Chambira Fm., Contamana, Peruvian Amazonia	Marivaux <i>et al.</i> (36); Antoine <i>et al.</i> (37)
<i>Branisella</i>	<i>boliviana</i>	late Oligocene	Deseadan SALMA	25.5	Uniform(26,25)	Salla, Level 5, Bolivia	Hoffstetter (38); Rosenberger (39); Takai and Anaya (40); Takai <i>et al.</i> (41)
<i>Antillothrix</i>	<i>bernensis</i> & (" <i>Insulacebus</i> ") <i>toussentiana</i>	Holocene	-	0.0-	Fixed(0)	Dominican Rep., Hispaniola	MacPhee and Woods (42); MacPhee <i>et al.</i> (43); Cooke <i>et al.</i> (44); Rosenberger <i>et al.</i> (45)
<i>Paralouatta</i>	<i>varonai</i>	Quaternary	-	0.0-	Fixed(0)	Cueva del Mono, Cuba	Rivero and Arredondo (46); Horovitz and MacPhee (47)
<i>Xenothrix</i>	<i>mcgregori</i>	Holocene	-	0.0-	Fixed(0)	Jamaica	Williams and Koopman (48); MacPhee and Horovitz (49)
<i>Parvimico</i>	<i>materdei</i>	early Miocene	Santacrucian SALMA	19-17	Uniform(17,19)	AMD-45, Bala Fm., Madre de Dios, Peruvian Amazonia	Kay <i>et al.</i> (50)
<i>Perupithecus</i>	<i>ucayaliensis</i>	early Oligocene	Tinguirirican	31,1-27,2	Uniform(27.2,31,1)	Santa Rosa, LACM loc. 6289, Yahuarango Fm., Peruvian Amazonia	Bond <i>et al.</i> (51); Campbell <i>et al.</i> (52)
<i>Ashaninkacebus</i>	<i>simpsoni</i>	late Eocene - early Oligocene	-	?	Uniform(13,45)*	PRJ-33, Rio Juruá, Bresilian Amazonia	This paper
<i>Ucayalipithecus</i>	<i>perdita</i>	early Oligocene	Tinguirirican	31,1-27,2	Uniform(27.2,31,1)	Santa Rosa, LACM loc. 6289, Yahuarango Fm., Peruvian Amazonia	Seiffert <i>et al.</i> (53); Campbell <i>et al.</i> (52)
<i>Hyllobates</i>	sp.	Extant	-	-	Fixed(0)	Indonesia	-

Taxa	species observed	Epoch or Interval (temporal range)	LMA	Age or range (Myr)	TRP - BTD (Myr)	Provenance(s)	References (figured or refigured observed material, and age information)
<i>Miopithecus</i>	<i>talapoin</i>	Extant	-	-	Fixed(0)	Africa	-
<i>Aegyptopithecus</i>	<i>zeuxis</i>	early Oligocene	Qatranian AFLMA	30-29.2	Uniform(29.2,30)	Quarries I/M, upper Jebel Qatrani Fm., Fayum Depression, Egypt	Simons (54–55); Kay <i>et al.</i> (56); Ankel-Simons <i>et al.</i> (57)
<i>Moeripithecus</i>	<i>markgrafi</i>	early Oligocene	Qatranian AFLMA	33.2-30.6	Uniform(30.6,33.2)	Taqah, Ashawq Fm., Dhofar, Sultanate of Oman	Thomas <i>et al.</i> (58)
<i>Catopithecus</i>	<i>browni</i>	latest Eocene	Phiomian AFLMA	35-34	Uniform(34,35)	L-41, lowermost Jebel Qatrani Fm., Fayum Depression, Egypt	Simons (59–61); Simons and Rasmussen (62)
<i>Oligopithecus</i>	<i>savagei & rogeri</i>	early Oligocene	Qatranian AFLMA	33.2-31	Uniform(31,33.2)	Quarry E, lower Jebel Qatrani Fm., Fayum Depression, Egypt; Taqah, Ashawq Fm., Dhofar, Sultanate of Oman	Simons (63); Rasmussen and Simons (64); Gheerbrant <i>et al.</i> (65)
<i>Talahpithecus</i>	<i>parvus</i>	late Eocene	Phiomian AFLMA	37-35	Uniform(35,37)	DT-Loc. 1, Bioturbated Unit, Dur At-Talah, Libya	Jaeger <i>et al.</i> (66)
<i>Amamria</i>	<i>tunisiensis</i>	late middle Eocene	Kebarian AFLMA	41-38	Uniform(38,41)	KEB-1, Djebel el Kébar, Tunisia	Marivaux <i>et al.</i> (3)
<i>Proteopithecus</i>	<i>sylviae</i>	latest Eocene	Phiomian AFLMA	35-34	Uniform(34,35)	L-41, lowermost Jebel Qatrani Fm., Fayum Depression, Egypt	Simons (59, 67–68); Miller and Simons (69); Simons and Seiffert (70)
<i>Biretia</i>	<i>piveteaui, fayumensis & megalopsis</i>	early late Eocene	Phiomian AFLMA	37.8-36.7	Uniform(36.7,37.8)	Bir el Ater, Algeria; BQ-2, Birket Qarun Fm., Fayum Depression, Egypt; DT-Loc. 1&2, Bioturbated Unit, Dur At-Talah, Libya	de Bonis <i>et al.</i> (71); Seiffert <i>et al.</i> (72); Jaeger <i>et al.</i> (66)
<i>Arsinoea</i>	<i>kallimos</i>	latest Eocene	Phiomian AFLMA	35-34	Uniform(34,35)	L-41, lowermost Jebel Qatrani Fm., Fayum Depression, Egypt	Simons (67)
<i>Serapia</i>	<i>eocaena</i>	latest Eocene	Phiomian AFLMA	35-34	Uniform(34,35)	L-41, lowermost Jebel Qatrani Fm., Fayum Depression, Egypt	Simons (67)
<i>Qatrania</i>	<i>wingi</i>	early Oligocene	Qatranian AFLMA	33.2-31	Uniform(31,33.2)	Quarry E, lower Jebel Qatrani Fm., Fayum Depression, Egypt	Simons and Kay (73–74)
<i>Parapithecus</i>	<i>fraasi</i>	early Oligocene	Qatranian AFLMA	35-29.2	Uniform(29.2,35)	Quarries I/M, Jebel Qatrani Fm., Fayum Depression, Egypt	Schlosser (75); Simons (76–78)
<i>Apidium</i>	<i>phiomense</i>	early Oligocene	Qatranian AFLMA	30-29.2	Uniform(29.2,30)	Quarries I/M, G/V, upper Jebel Qatrani Fm., Fayum Depression, Egypt	Osborn (79); Simons (61, 63); Fleagle and Simons (80)
<i>Simonsius</i>	<i>grangeri</i>	early Oligocene	Qatranian AFLMA	30-29.2	Uniform(29.2,30)	Quarries I/M, upper Jebel Qatrani Fm., Fayum Depression, Egypt	Schlosser (75); Simons (78)
<i>Myanmarpithecus</i>	<i>yarshensis</i>	late middle Eocene	Sharamurunian ALMA	40-38	Uniform(38,40)	Yarshe, Pondaung Fm., Myanmar	Takai <i>et al.</i> (81)
<i>Ganlea</i>	<i>megacanina</i>	late middle Eocene	Sharamurunian ALMA	40-38	Uniform(38,40)	Ganle, Than-U-Do, Pondaung Fm., Myanmar	Beard <i>et al.</i> (82); Jaeger <i>et al.</i> (83)
<i>Pondaungia / Amphipithecus</i>	<i>cotteri & mogaungensis</i>	late middle Eocene	Sharamurunian ALMA	40-38	Uniform(38,40)	Pondaung Fm., Myanmar	e.g., Colbert (84); Chaimanee <i>et al.</i> (85); Ciochon <i>et al.</i> (86); Ciochon and Gunnell (87); Coster <i>et al.</i> (88)
<i>Siamopithecus</i>	<i>eocaenus</i>	latest Eocene	Ergilian ALMA	35.5-33	Uniform(33,35.5)	Bang Mark Lignite Mine, Krabi, Thailand	Chaimanee <i>et al.</i> (89–90); Ducrocq (91); Zollikofer <i>et al.</i> (92)
<i>Bugtipithecus</i>	<i>inexpectens</i>	early Oligocene	Hsandagolian ALMA	33.9-28	Uniform(28,33.9)	DBC2, Bugti Hills, Chitarwata Fm., Balochistan, Pakistan	Marivaux (5); Marivaux <i>et al.</i> (93)

Taxa	species observed	Epoch or Interval (temporal range)	LMA	Age or range (Myr)	TRP - BTD (Myr)	Provenance(s)	References (figured or refigured observed material, and age information)
<i>Phileosimias</i>	<i>kamali</i>	early Oligocene	Hsandagolian ALMA	33.9-28	Uniform(28,33.9)	DBC2, Bugti Hills, Chitarwata Fm., Balochistan, Pakistan	Marivaux (5); Marivaux <i>et al.</i> (93)
<i>Eosimias</i>	<i>centennicus</i>	late middle Eocene	Sharamurunian ALMA	41.2-37.8	Uniform(37.8,41.2)	Heti Fm., China	Beard <i>et al.</i> (94–95); Tong (96); Beard and Wang (97)
<i>Bahinia</i>	<i>pondaungensis</i>	late middle Eocene	Sharamurunian ALMA	40-38	Uniform(38,40)	Yarshe, Pondaung Fm., Myanmar	Jaeger <i>et al.</i> (98)
<i>Bahinia</i>	<i>banyueae</i>	early Oligocene	Hsandagolian ALMA	33.9-32	Uniform(32,33.9)	Lijiwa fossil site, upper Caijiachong Fm.	Ni <i>et al.</i> (99)
<i>Phenacopithecus</i>	<i>krishtalkai & xueshii</i>	late middle Eocene	Sharamurunian ALMA	41.2-37.8	Uniform(37.8,41.2)	Nanbaotou, Heti Fm., Henan Province, China	Beard and Wang (97)
<i>Afrotarsius</i>	<i>chatrathi & libycus</i>	late Eocene - earliest Oligocene	Phiomian/Qatranian AFLMA	37-29.2	Uniform(29.2,37)	Quarry M, Jebel Qatrani Fm., Fayum Depression, Egypt; DT-Loc. 1, Bioturbated Unit, Dur At-Talah, Libya	Jaeger <i>et al.</i> (66); Simons and Bown (100); Chaimanee <i>et al.</i> (101)
<i>Afrasia</i>	<i>djijidae</i>	late middle Eocene	Sharamurunian ALMA	40-38	Uniform(38,40)	Nyaungpinle, Pondaung Fm., Myanmar	Chaimanee <i>et al.</i> (101)
<i>Tarsius</i>	<i>spectrum</i>	Extant	-	-	Fixed(0)	Sulawesi	-
<i>Xanthorhysis</i>	<i>tabrumi</i>	late middle Eocene	Sharamurunian ALMA	41.2-37.8	Uniform(37.8,41.2)	Heti Fm., Shanxi Province, China	Beard (102)
<i>Teilhardina</i>	<i>belgica</i>	earliest Eocene	MP7	55.8-55.4	Uniform(55.4,55.8)	Dormaal, Belgium	Szalay and Delson (4); Teilhard de Chardin (103)
<i>Hemiacodon</i>	<i>gracilis</i>	middle Eocene	Bridgerian NALMA	48-46	Uniform(46,48)	Four Mile, Rocky Mountain, USA	Szalay and Delson (4); Marsh (104)
<i>Tetonius</i>	<i>homunculus</i>	earliest Eocene	Wasatchian NALMA	54.8-54.4	Uniform(54.4,54.8)	Upper Bridger, Rocky Mountain, USA	Szalay and Delson (4); Matthew (105)
<i>Leptadapis</i>	<i>magnus</i>	late Eocene	MP17-MP19	38-35	Uniform(35,38)	Quercy Ph., Fons, Euzet, France	Szalay and Delson (4); Filhol (106); Gervais (107); UM Collections
<i>Adapis</i>	<i>parisiensis</i>	late Eocene	MP16-MP19	38-35	Uniform(35,38)	Quercy Ph. (Escamps, Rosières), Robiac, France	Szalay and Delson (4); Cuvier (108); UM Collections
<i>Djebelemur</i>	<i>martinezi</i>	latest early / earliest middle Eocene	Lazibian AFLMA	50-45	Uniform(45,50)	CBI-1, Chambi, Tunisia	Hartenberger and Marandat (109); Marivaux <i>et al.</i> (110)
<i>Eulemur</i>	<i>fulvus</i>	Extant	-	-	Fixed(0)	Madagascar	-
<i>Varecia</i>	<i>variegata</i>	Extant	-	-	Fixed(0)	Madagascar	-
<i>Loris</i>	<i>tardigradus</i>	Extant	-	-	Fixed(0)	India	-

Fm.: Formation

LMA: Land Mammal Ages

AFLMA: African Land Mammal Ages

ALMA: Asian Land Mammal Ages

MP: European Mammal Paleogene

TRP - BTD : Temporal range priors for Bayesian tip-dating analyses (Upper and lower bounds of each uniform age prior)

*: broad temporal range prior (age considered as unknown)

Table S2. Summary of the different types of analyses (A1 to A6) performed to investigate the phylogenetic position of *Ashaninkacebus simpsoni* gen. et sp. nov. in a high-level phylogeny of basal anthropoids from the Old World (i.e., Paleogene South Asian and North African known taxa), plus known extinct and extant New World platyrrhines (see Table S1). We performed a cladistic assessment of the morphological evidence, as well as Bayesian tip-dating (BTD) analyses on the same morphological dataset to estimate divergence times between taxa (and also both, i.e., phylogeny and divergence times). Below are summarized the topological constraints applied to the analyses.

n°	A	Topological constraints	Additional constraint (assessment)	Dataset	Figure	
A1	PAUP 4.0a 169	MP	Molecular backbone of extant primates	-	S2	S5
A2	Mesquite 3.61	-	Molecular backbone of extant primates	Amphipithecidae as stem anthropoids (<i>sensu</i> ref. 53 and 83)	-	S6
A3	MrBayes 3.2.7a	BTD	PAUP tree of A1 (HC)	-	S3	S7
A4	MrBayes 3.2.7a	BTD	Mesquite tree of A2 (HC)	Amphipithecidae as stem anthropoids (as in A2)	S4	S8
A5	MrBayes 3.2.7a	BTD	Molecular backbone of extant primates (PC) + branching groups of Anthropoidea and outgroups of A1 (HC)	-	S4	S9
A6	MrBayes 3.2.7a	BTD	Molecular backbone of extant primates (PC) + branching groups of Anthropoidea and outgroups of A1 (HC)	Amphipithecidae as stem anthropoids (as in A2)	S4	S10

A: Analysis (type of analysis)
 MP: Maximum Parsimony (via Heuristic searches [Hsearch])
 BTD: Bayesian tip-dating
 HC: Hard constraint
 PC: Partial constraint

Text S2. The Bayesian tip-dating (BTD) approach was performed primarily to estimate divergence times between taxa (notably for A3 and A4, in which the parsimony-based topologies of A1 and A2 were applied as hard constraints, respectively). However, we also performed a BTD analysis (A5) with no topological constraints employed within the Anthropoidea clade, other than those of a molecular scaffold for extant primates, and those of the Anthropoidea branching-groups and outgroups. We duplicated the latter BTD analysis (A5), in evaluating the impact of considering (as in A4) the Amphipithecidae clade as stem Anthropoidea (A6). In our matrix, “multistate taxa” were considered for some characters. In these cases, characters were scored primarily as polymorphic (e.g., 0 and 1; i.e., 0+1: morphological variability in a given species) or as uncertain (e.g., 0 or 1; i.e., 0/1: when a character state observed in a species/individual was ambiguous). Unlike PAUP, which treats distinctly polymorphic (**01**) under PAUP) *versus* uncertain (**01**) under PAUP), character states (options MSTaxa = Variable), MrBayes (v. 3.2.7a) treats all cases of polymorphism and uncertainty in the matrix as missing data (i.e., “?”). In our matrix, more than 4% of scores for the dental characters are polymorphic (418) and uncertain (560) states, dental **scores that are then lost** in the different BTD analyses. In cases A5 and A6, where the phylogeny is estimated by a Bayesian approach, the position of poorly-sampled taxa, which may moreover include uncertain and polymorphic character states (*ipso facto* discarded), can be then strongly impacted and irrelevant.

A1

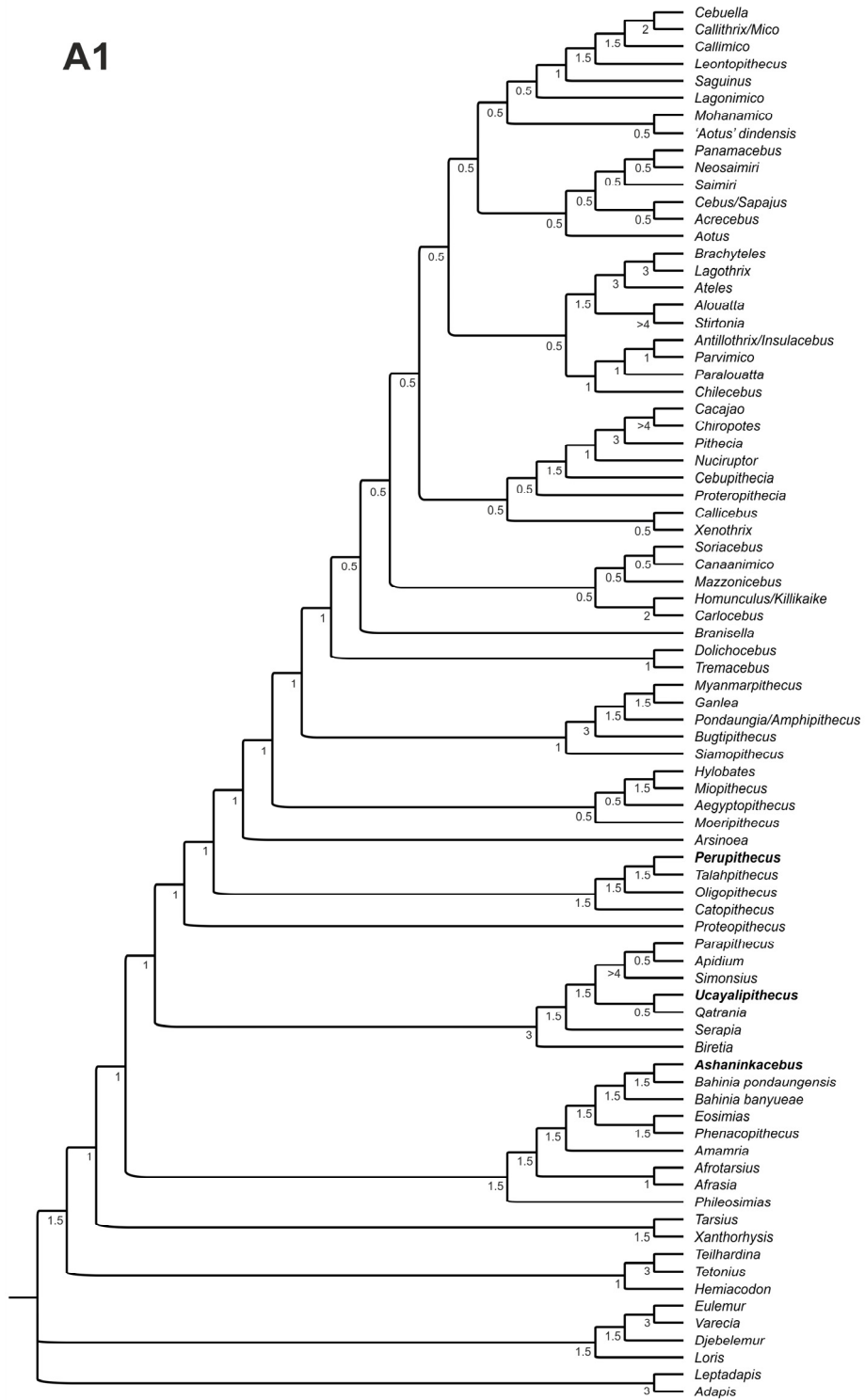


Fig. S5. Results of the A1 analysis. Phylogenetic position of *Ashaninkacebus simpsoni* gen. et sp. nov. Single most-parsimonious tree of 2429.49 steps (Consistency index [CI] = 0.358; Retention index [RI] = 0.556). Bremer (B) values are indicated by the numbers labelled under internal branches (B ≥ 0.5).

A2

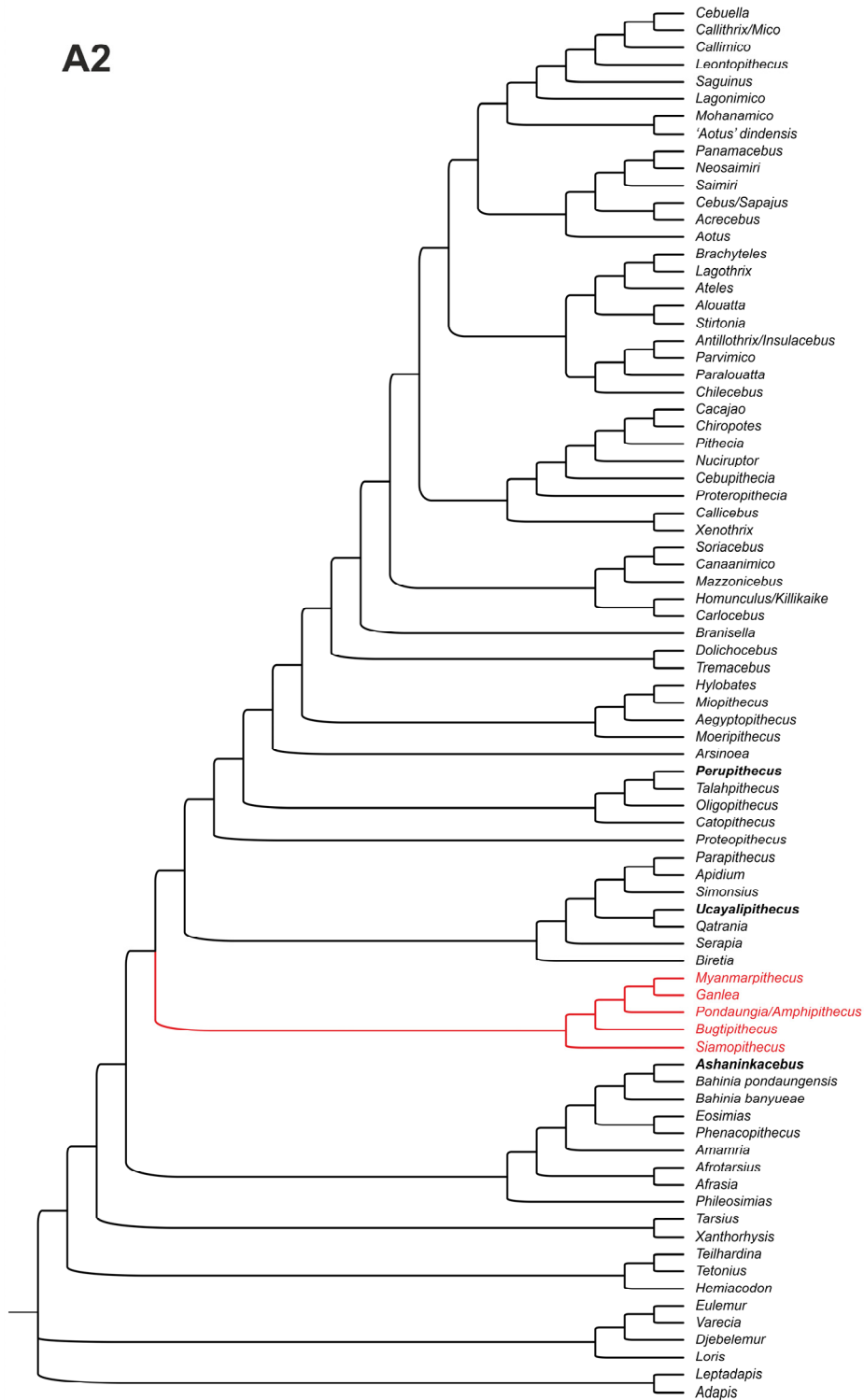


Fig. S6. Results of the A2 analysis. Phylogenetic tree of A1, but with the Amphipithecidae clade (in red) placed as stem Anthropoidea (*sensu* ref. 53 and 83). This position change requires about 12 additional steps (A2 tree of 2441.81 steps; CI = 0.356; RI = 0.553) over the most-parsimonious A1 tree (Fig. S5).

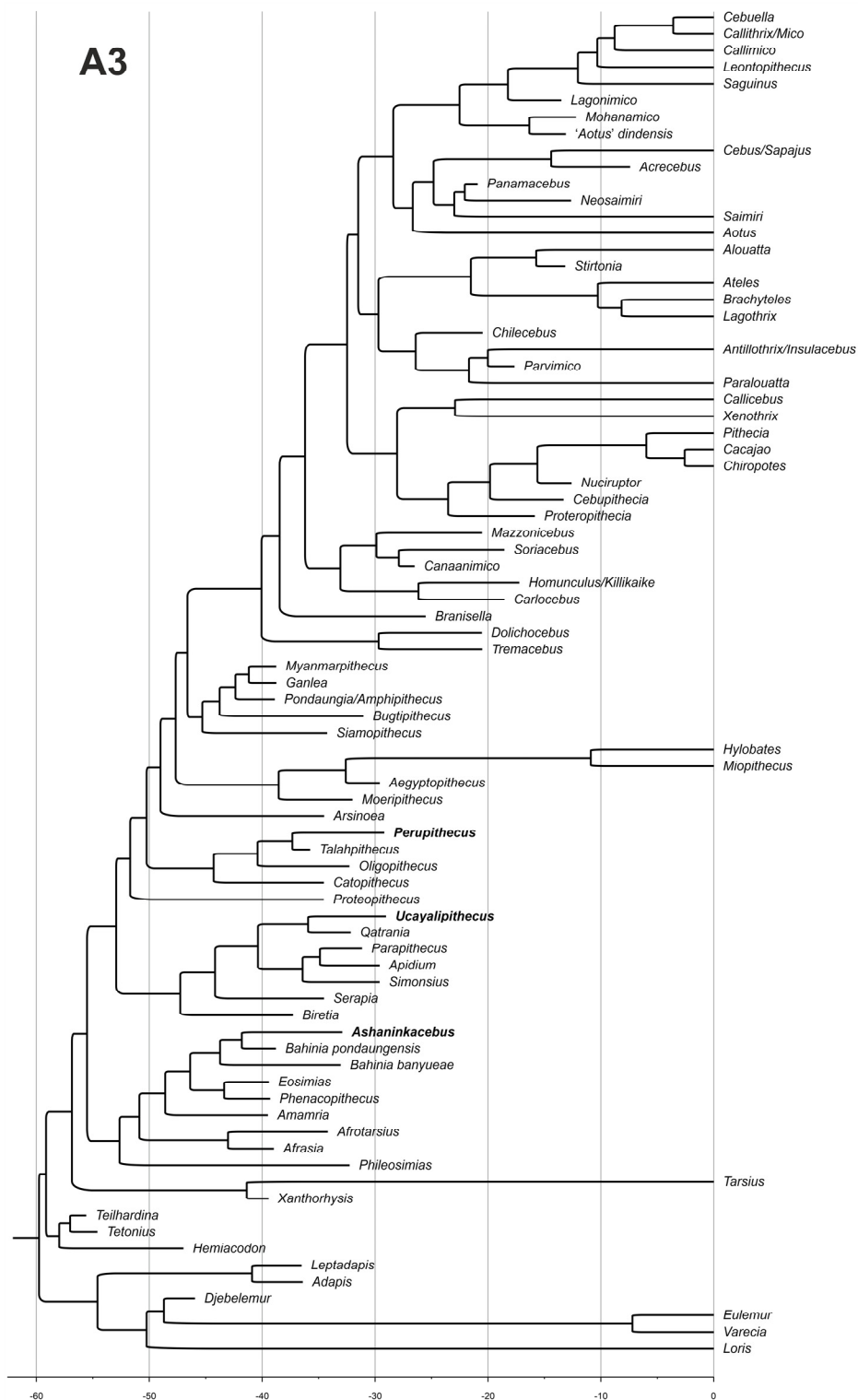


Fig. S7. Results of the A3 analysis (see [Tables S2 and S3](#)). The phylogenetic tree of A1 was subjected to a Bayesian morphological clock analysis (Bayesian tip-dating [BTD]) to estimate divergence times between taxa (see also [Table S4](#)). This tree is that presented in the article (Fig. 2).

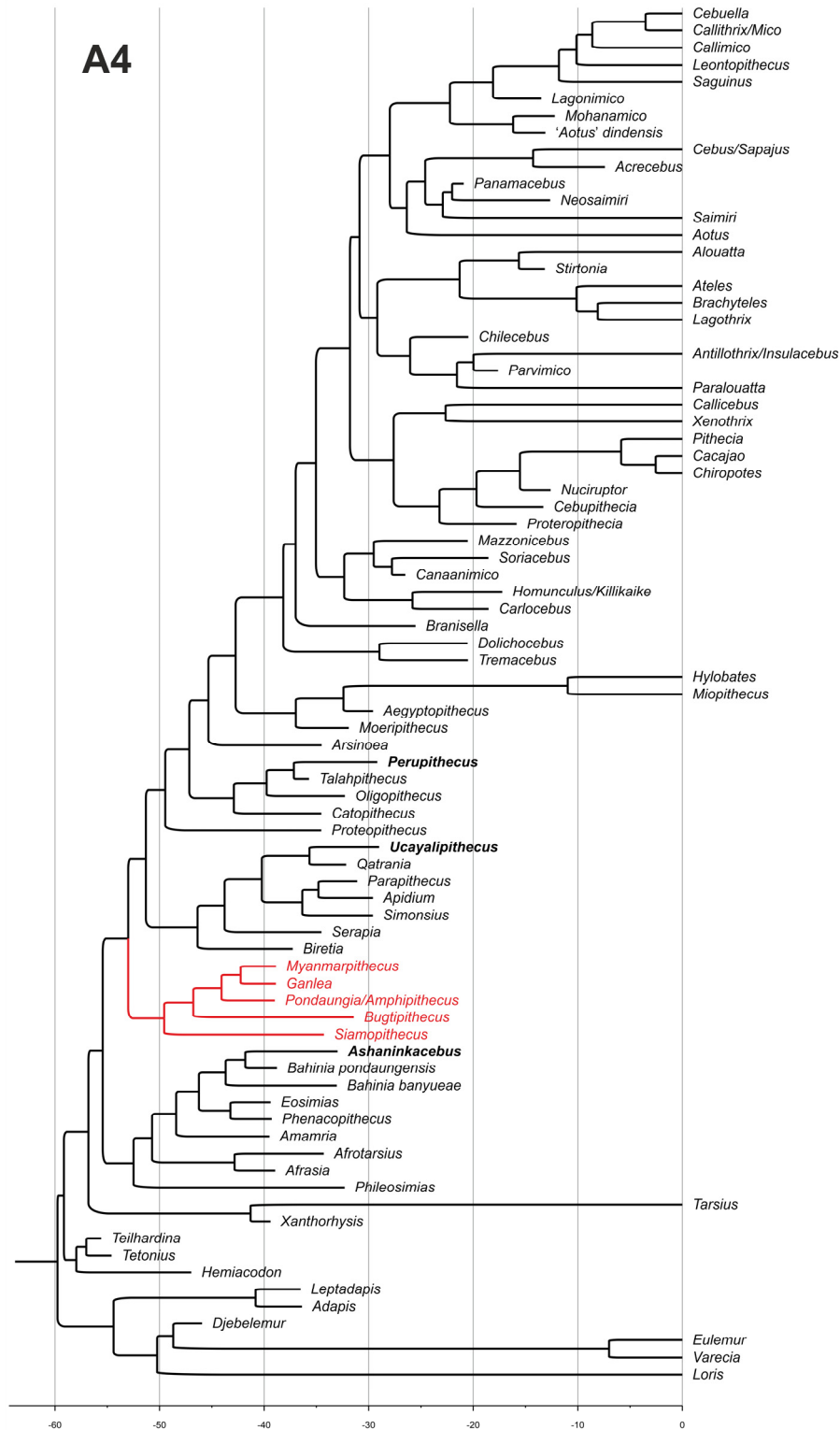


Fig. S8. Results of the A4 analysis (see [Tables S2 and S3](#)). The phylogenetic tree of A2 (Amphipithecidae clade [in red] placed as stem Anthropoidea) was subjected to a Bayesian tip-dating (BTD) analysis to estimate divergence times between taxa (see also [Table S4](#)).

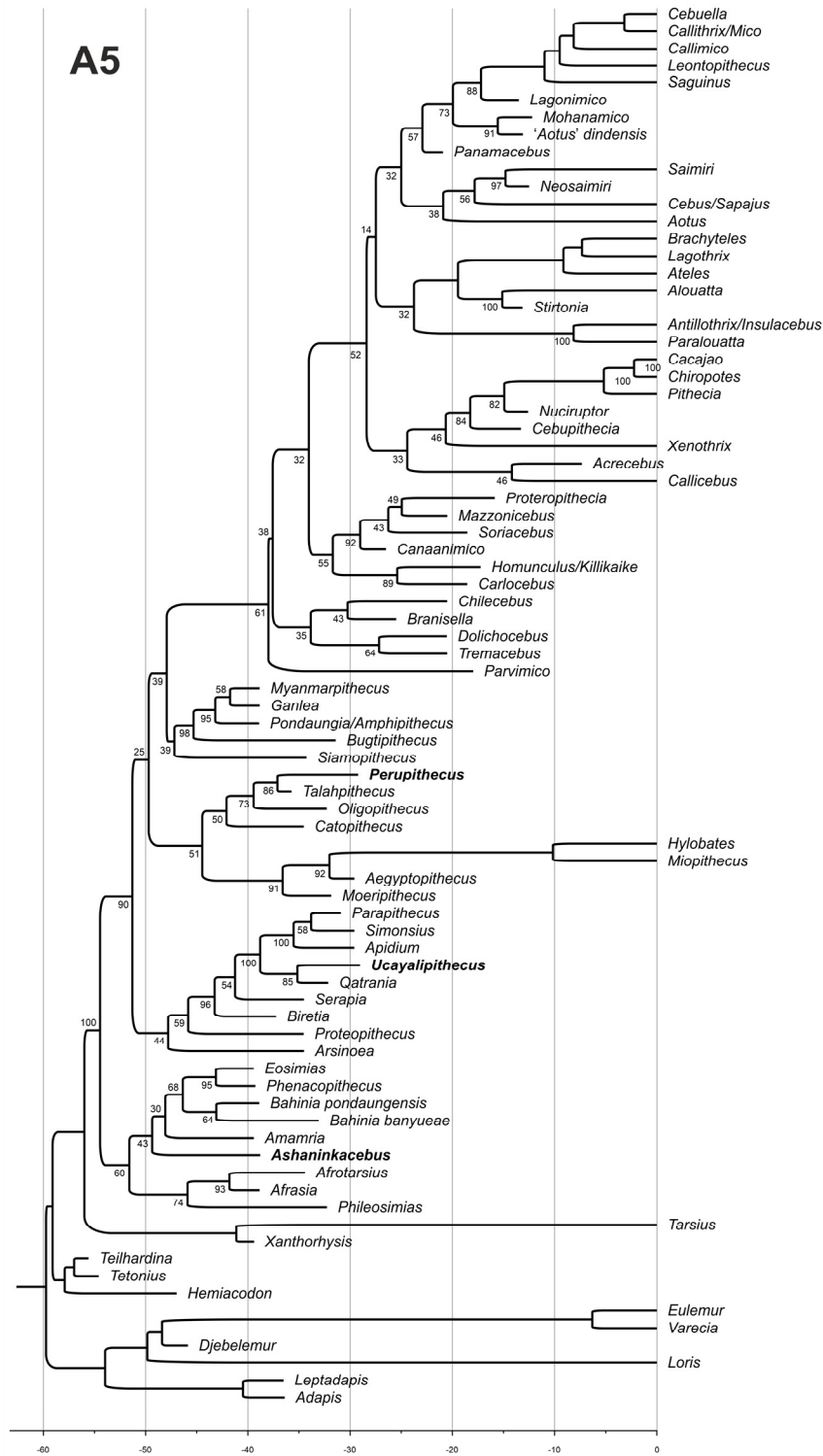


Fig. S9. Results of the A5 analysis (see Table S2 for limited constraints applied). “Allcompat” consensus tree (majority-rule plus compatible groups) of 50,000 post-burn-in trees retained (see Table S3). Number at each node is the posterior probability ($\times 100$) for each node on the basis of the Bayesian clock analysis. See Table S4 for comparisons of some age estimates.

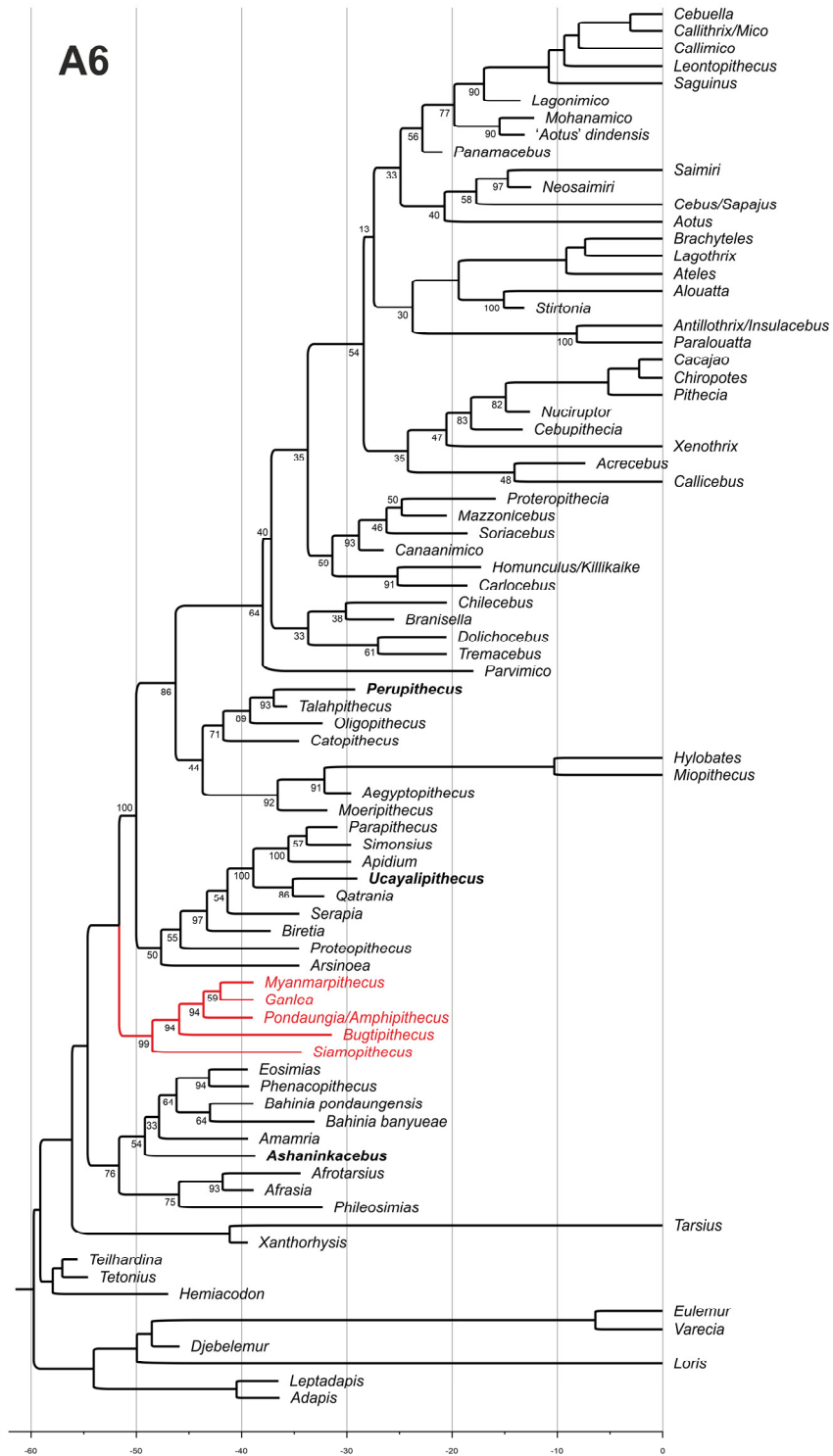


Fig. S10. Results of the A6 analysis (see [Table S2](#) for constraints applied). “Allcompat” consensus tree of 50,000 post-burn-in trees retained (see [Table S3](#)). Number at each node is the posterior probability ($\times 100$) for each node on the basis of the Bayesian clock analysis. See [Table S4](#) for comparisons of some age estimates.

Table S3. Statistics associated to the results of the Bayesian tip-dating analyses (A3 to A6).

ESS: Effective sample size.

PSRF: Potential Scale Reduction Factor (Convergence diagnostic should approach 1.0 as runs converge).

A3

Summary Statistic	Median	95% HPD Interval	ESS	PSRF
LnL	-11089.14	[-11107.89, -11071.53]	23084.6484	-
LnPr	-759.2051	[-799.4894, -718.0193]	3215.8974	-
TH	12.4059	[6.1532, 18.3655]	8640.3203	1.000
TL	232.8076	[116.6567, 348.9945]	8045.4084	1.000
alpha	1.1901	[1.0304, 1.3631]	83330.6743	1.000
m{1}	0.0924	[0.0519, 0.1638]	4938.3385	1.000
net_speciation	0.029	[7.9689E-3, 0.0517]	13844.7939	1.005
relative_extinction	0.996	[0.9889, 0.9997]	1679.2302	1.014
relative_fossilization	7.0941E-5	[6.1389E-6, 2.6801E-4]	1545.3513	1.015
igrvar	0.8365	[0.3896, 1.3228]	9056.3579	1.000
clockrate	0.2079	[0.1028, 0.3074]	8632.431	1.000

Summary statistics for partitions with frequency ≥ 0.10 in at least one run:

Average standard deviation of split frequencies = 0.000001

Average PSRF for parameter values (excluding NA and >10.0) = 1.000

A4

Summary Statistic	Median	95% HPD Interval	ESS	PSRF
LnL	-11096.76	[-11115.41, -11079.33]	24723.0537	-
LnPr	-748.244	[-787.5277, -706.6717]	7575.2792	-
TH	12.5212	[6.5016, 18.5093]	9568.2134	1.000
TL	230.0393	[118.5485, 342.9195]	8277.9555	1.000
alpha	1.1808	[1.019, 1.352]	80649.1969	1.000
m{1}	0.0938	[0.0531, 0.1623]	6271.0331	1.000
net_speciation	0.0286	[7.032E-3, 0.0508]	17360.5494	1.000
relative_extinction	0.9964	[0.9899, 0.9999]	20666.0945	1.000
relative_fossilization	5.9426E-5	[5.1674E-6, 2.3581E-4]	34216.8647	1.000
igrvar	0.7994	[0.3905, 1.2612]	10185.63	1.000
clockrate	0.2099	[0.1095, 0.3108]	9575.0167	1.000

Summary statistics for partitions with frequency ≥ 0.10 in at least one run:

Average standard deviation of split frequencies = 0.000010

Average PSRF for parameter values (excluding NA and >10.0) = 1.000

A5

Summary Statistic	Median	95% HPD Interval	ESS	PSRF
LnL	-11087.02	[-11109.05, -11066.66]	8093.5821	-
LnPr	-717.6052	[-758.8796, -677.357]	1165.1557	-
TH	12.824	[6.9239, 18.9277]	10893.7437	1.000
TL	218.8289	[115.0353, 323.6273]	10108.3743	1.000
alpha	1.1568	[0.9979, 1.3246]	55095.6652	1.000
m{1}	0.0998	[0.0591, 0.1716]	7773.1855	1.000
net_speciation	0.0273	[5.251E-3, 0.053]	1469.2552	1.013
relative_extinction	0.9976	[0.6985, 1]	303.769	1.117
relative_fossilization	3.5132E-5	[2.2666E-6, 0.5099]	323.2909	1.109
igrvar	0.6941	[0.3391, 1.1023]	10009.614	1.000
clockrate	0.2151	[0.1174, 0.3185]	10917.4378	1.000

Summary statistics for partitions with frequency ≥ 0.10 in at least one run:
Average standard deviation of split frequencies = 0.008697
Average PSRF for parameter values (excluding NA and >10.0) = 1.000

A6

Summary Statistic	Median	95% HPD Interval	ESS	PSRF
LnL	-11087.8	[-11108.8, -11067.13]	13143.2867	-
LnPr	-714.5596	[-751.9399, -676.4803]	6088.7483	-
TH	12.9008	[6.8265, 18.9326]	10873.9426	1.000
TL	219.1573	[113.6311, 322.836]	9510.3708	1.001
alpha	1.1629	[1.0056, 1.3342]	74632.4188	1.000
m{1}	0.0998	[0.0576, 0.1711]	4606.7612	1.001
net_speciation	0.0262	[5.4294E-3, 0.0483]	15877.2456	1.000
relative_extinction	0.9977	[0.9943, 0.9998]	15786.9298	1.000
relative_fossilization	3.3045E-5	[5.1037E-6, 9.5001E-5]	23106.3028	1.000
igrvar	0.6744	[0.3242, 1.0736]	6246.4896	1.003
clockrate	0.2163	[0.1139, 0.3168]	10894.1556	1.000

Summary statistics for partitions with frequency ≥ 0.10 in at least one run:
Average standard deviation of split frequencies = 0.017412
Average PSRF for parameter values (excluding NA and >10.0) = 1.001

For the whole analyses (A3 to A6), all criteria have good ESS and PSRF values, thereby indicating that all of the BTD analyses were of sufficient duration to ensure that parameters were sufficiently sampled (i.e., the convergence was reached).

Table S4. Median age estimates for *Ashaninkacebus simpsoni* gen. et sp. nov. and comparisons of median age estimates for the divergence between some taxa of interest mentioned in the main text. These median age estimates derive from the different types of Bayesian tip-dating (BTD) analyses (A3 to A6). Age estimates are in Mega-annum (Ma).

	A3		A4		A5		A6	
	Median age	HPD	Median age	HPD	Median age	HPD	Median age	HPD
<i>Ashaninkacebus simpsoni</i>	32.9	42.1–19.9	32.9	42.3–20.2	38.8	45.0–25.8	38.7	45.0–25.7
<i>Ashaninkacebus/Bahinia p.</i>	41.8	45.5–38.9	41.8	45.31–38.9	-	-	-	-
<i>Ashaninkacebus/Eosimiidae</i>	-	-	-	-	49.3	53.4–45.3	49.2	53.2–45.2
<i>Ucayalipithecus/Qatrania</i>	35.9	40.6–32.0	35.6	40.1–32.0	35.16	39.0–32.0	35.1	39.0–31.9
<i>Perupithecus/Talahpithecus</i>	37.3	40.3–35.3	37.1	39.8–35.3	37.1	40.1–35.2	36.9	39.3–35.2
Stem Platyrrhini	40.0	44.9–35.5	38.1	42.4–34.2	38.0	43.4–33.2	38.0	43.8–33.1
Crown Platyrrhini	32.5	36.5–28.7	31.8	35.5–28.4	28.4	32.4–24.7	28.4	32.7–24.7

HPD: 95% highest posterior density

Text S3. A summary of the different types of analyses performed (A1 to A6) is provided in [Table S2](#). The section “*Materials and Methods*” of the main text provides details of all the parameters employed for each analysis. All the statistics associated to the results of the different BTD analyses (A3 to A6) are provided in [Table S3](#). We describe below the resulting topology of each analysis, and compare the estimated median ages resulting from the BTD analyses ([Table S4](#)).

Comments: We think that phylogenetic relationships of extinct taxa should be based solely on morphology (shared derived characters), and not be influenced by the age of the taxa. Also, according to us, a Bayesian tip-dating (BTD) approach should be performed primarily to estimate divergence times between taxa, but only based on a fixed topology obtained by another approach, i.e., with age-free phylogenetic relationships. Many molecular-based studies adopt such a two-step procedure with a topology estimation first, followed by a dating inference in which the topology is fixed with the obtained tree in the first step (111, 112). Furthermore, it is worth mentioning that temporal-paralogy biases are a strong issue (113, 114), not fully solved through probabilistic approaches, such as BTD. For these reasons and also because MrBayes treats all cases of polymorphism and uncertainty as missing data (see [Text S2](#)), we decided to only present in the main text of our article the A1 PAUP topology (Fig. 2), which was constrained *in extenso* for a BTD analysis (A3), the latter for the “sole” purpose of estimating divergence times between taxa. However, we also provide here results of “unconstrained” (partially constrained; see [Table S2](#)) BTD analyses (A5 and A6) for comparative purposes.

Results of the A1 analysis: The analyses yielded a single most-parsimonious tree (2429.49 steps, Consistency index = 0.36; Retention index = 0.56; [Fig. S5](#)). The cladogram shows that the three oldest known primates from the early Oligocene of South America are not related to later platyrrhine monkeys but are nested within three distinct clades of Old World basal anthropoids. *Ashaninkacebus* is nested within the Eosimiidae clade (sister to *Bahinia*), *Perupithecus* within the Oligopithecidae clade (sister to *Talahpithecus*), and *Ucayalipithecus* is nested within the Parapithecidae clade (sister to *Qatrania*) as formerly resolved by Seiffert et al. (53). Within Platyrrhini, we recover a pattern underscoring a stem radiation *versus* a crown radiation (34, 115), with, however, some changes regarding the Pleistocene Caribbean taxa (*Antillothrix/Insulacebus*, *Paralouatta*, and *Xenothrix*). The latter were previously resolved as stem platyrrhines (36, 115), but are interpreted here as crown platyrrhines. For the analysis, we have

constrained the phylogenetic position of *Xenothrix* close to the Callicebinae, inasmuch as ancient DNA analyses recently demonstrated its pitheciid affinities (116). In contrast, *Paralouatta* and *Antillothrix/Insulacebus*, along with *Parvimico* and *Chilecebus*, are here resolved as a sister clade to the Atelidae, or stem Atelidae [as originally proposed for *Paralouatta* (46)], but see Kay et al. (50, 115) for different results regarding these aforementioned taxa.

The question of the Amphipithecidae. Within Euprimates, the high-level phylogenetic position of the South Asian Paleogene Amphipithecidae has long been the subject of much debates (for a summary of bibliographic references, see ref. 117–119). Thanks to continuous field efforts, new paleontological data collected over the last 20 years have strengthened support for the hypothesis of their anthropoid status. However, the position of the Amphipithecidae within the Anthropoidea clade has been in a state of flux over the last decade (stem *versus* close to or crown anthropoids; e.g., ref. 5, 82, 83, 93, 101, 119, 120). From our phylogenetic results in maximum parsimony (MP), Amphipithecidae branch out quite high in the Anthropoidea clade, and are surprisingly resolved as closely related to Platyrrhini. However, this relationship is not strongly supported (Bremer support of 1), which means that this branching pattern relies on few morphological character states. The concerned characters are dental, being related to the configuration of the “hypometacrista complex” and orientation of the postprotocrista, which are similarly arranged in amphipithecids and in extinct and extant platyrrhines, but perhaps due to convergent evolutionary paths. A stem anthropoid status of the Amphipithecidae has recently gained significant support, thanks to the discovery of a cranial fragment referred to as *Ganlea megacanina* from the upper middle Eocene Pondaung Formation in Myanmar (83). This cranial fragment includes parts of the frontal and parietal bones, some subtle traits of which allowed Jaeger et al. (83) to suggest that this taxon (and by extension its closely-related amphipithecid taxa) did not display a postorbital closure (the presence of a postorbital closure being a character of advanced stem anthropoids and crown anthropoids). For our phylogenetic analyses, we included in our morphological matrix as many cranial characters as could be coded from the cranial material documenting *Ganlea*. In Jaeger et al. (83), this postorbital condition known/interpreted for *Ganlea* (i.e., lack of postorbital closure) was optimized for all other amphipithecid taxa, and extrapolated as a symplesiomorphic trait. From our MP results, this postorbital condition known/interpreted for *Ganlea* (i.e., lack of postorbital closure), was interpreted as an autapomorphic reversal trait in *Ganlea* (the presence or absence of a postorbital closure in all other amphipithecids is equivocal, but optimized as present). Considering our phylogenetic results resolving the amphipithecids more derived than expected within the Anthropoidea clade, these results would suggest that *Ganlea* (and perhaps all amphipithecids by extension) has lost the postorbital closure, a fact hardly conceivable and even unlikely.

Results of the A2 analysis: We assessed the impact of constraining the Amphipithecidae clade in a more basal position within the Anthropoidea clade [i.e., stem anthropoids, diverging after the Eosimiiformes; *sensu* Jaeger et al. (83) or even Seiffert et al. (53)]. We found that such a topology (Fig. S6) requires 12 additional steps with respect to the results of the A1 analysis (Fig. S5).

Results of the A3 analysis: The resulting MP A1 tree topology was used for a Bayesian tip-dating (BTD) analysis to estimate divergence times between taxa, not the phylogeny via a Bayesian approach (Fig. S7). All nodes of the cladogram were thus applied as hard constraints for the BTD analysis. The BTD analysis with *Ashaninkacebus* assigned to a broad age prior, returned a median age of ≈ 32.9 Ma (95% HPD = 42.1–19.9 Ma) for this new taxon (Table S4), an age that is consistent with the biochronological inferences derived from the caviomorph rodents

(Fig. S2) found in association at PRJ-33' (i.e., nearby the Eocene/Oligocene transition, ca. 34 Ma). Also of interest are the divergence-time estimates of the three ancient primates (*Perupithecus*, *Ucayalipithecus*, and *Ashaninkacebus*) found in South America from their Old World counterparts (Table S4), estimates which can be traced back to the late middle–late Eocene for *Perupithecus* (≈ 37.33 Ma, 95% HPD = 40.3–35.3 Ma), to the late middle Eocene–earliest Oligocene for *Ucayalipithecus* (≈ 35.93 Ma, 95% HPD = 40.6–32.0 Ma), and to the middle–late Eocene for *Ashaninkacebus* (≈ 41.8 Ma, 95% HPD = 45.5–38.9 Ma). Here, the crown platyrrhine radiation is traced back to the early Oligocene, resulting in a substantial incompleteness of the fossil record, while the stem platyrrhine radiation is estimated to extend back to the late middle Eocene (Fig. S7; Table S4). The latter estimates are close to some extent with the divergence-time estimates of the early known South American primate fossils from their Old World counterparts, although no phylogenetic relationship can be formally established between *Ashaninkacebus* or *Perupithecus* and the stem platyrrhines yet.

Results of the A4 analysis: We performed the same BTM analysis than the A3 analysis, but in applying as hard constraints all nodes of the A2 tree, which places the Amphipithecidae clade at a more basal position within the Anthropeidea clade (i.e., stem anthropoids, diverging after the Eosimiiformes; ref. 53 and 83). This BTM analysis returns a similar median age of ≈ 32.9 Ma (95% HPD = 42.3–20.2 Ma; Fig. S8; Table S4) for *Ashaninkacebus*. The divergence-time estimates of the three ancient primates found in South America (*Ashaninkacebus*, *Perupithecus*, and *Ucayalipithecus*) with their Old World counterparts remain unchanged from those of the A3 analysis (see Table S4). Only the stem platyrrhine radiation, although still old (late middle Eocene), is here traced slightly more recently (about 2 million years younger; Table S4), while the crown platyrrhine radiation is estimated to date similarly to the early Oligocene (Table S4). The more basal placement of the Amphipithecidae clade has practically no effect on the morphological clock analysis for estimating divergence times between taxa.

Results of the A5 analysis: With this BTM analysis, we estimated simultaneously phylogenetic topology and divergence times of taxa (but see our comments above regarding our reluctance to incorporate fossil ages into phylogenetic reconstruction). MrBayes treats all cases of polymorphism and uncertainty as missing data (see Text S2). In that context, several morphological scores were then discarded, a loss of information that can have impacted the phylogenetic reconstruction, and provided irrelevant position of some taxa. Although the overall tree topology of these results (Fig. S9) is not in conflict with that deriving from the PAUP results (A1, Fig. S5), there are, however, phylogenetic changes regarding a number of taxa. *Ashaninkacebus* is retrieved among the Eosimiiformes, but occupying a more basal position, resolved as the earliest offshoot of the Eosimiidae clade. This stemward phylogenetic position of *Ashaninkacebus* in the Eosimiidae has an implication for its corresponding estimated median age, which is set back more than 6 million years (≈ 38.8 Ma; 95% HPD = 45.0–25.8 Ma; see Table S4). Such an old age is otherwise inconsistent with the biochronological inferences assembled from PRJ-33'. Besides, the divergence-time estimate of *Ashaninkacebus* from other eosimiids is incredibly old (≈ 49.3 Ma; 95% HPD = 53.4–45.3 Ma; see Table S4) and somewhat unlikely. *Perupithecus* and *Ucayalipithecus* are resolved similarly than with the MP A1 analyses (i.e., sister-group to *Talahpithicus* and *Qatrania*, respectively), and with divergence-time estimations from their respective African counterparts, as previously computed (A3; see Table S4). Among Platyrrhini, within the Cebidae clade, *Panamacebus* is resolved as the earliest offshoot of the Callitrichinae clade (Fig. S9), rather than being nested within the Cebinae clade (sister to *Neosaimiri*) as previously resolved in the A1 tree (Fig. S5). In contrast, *Acrecebus*, previously retrieved as sister taxon to *Cebus/Sapajus* within the Cebinae (Fig. S5; in agreement with Kay

and Cozzuol, ref. 9), is here found among the Pitheciidae, as sister to *Callicebus* (Fig. S9). *Proteropithecina*, originally described as a stem Pitheciidae (16, 17), and previously retrieved as such (Fig. S5), is here resolved among the Homunculidae (i.e., stem Platyrrhini), and closely related to *Mazzonicebus* (Fig. S9). *Parvimico* is resolved as the earliest offshoot of the Platyrrhini clade (Fig. S9), whereas it was found closely related to *Antillothrix* in the A1 tree, in a clade sister to Atelidae (Fig. S5). An almost similar situation is observed for *Chilecebus*, which is resolved here as a stem platyrrhine (closely related to *Branisella*; Fig. S9), whereas it was resolved as belonging to the clade sister to Atelidae (as *Parvimico*) in the A1 tree (Fig. S5). *Acrecebus*, *Proteropithecina* and *Parvimico* are very poorly documented taxa, and the “uncertainty” scores for some character states (not considered by MrBayes) may have strongly affected their phylogenetic placement in this BTM analysis. From this analyses, the crown and stem platyrrhine radiations are estimated to have occurred slightly more recently than previously found in the A3 analysis (Table S4). The crown platyrrhine radiation is here traced back to the late early Oligocene (so about 2 million years younger than previously; see A3), while the stem platyrrhine radiation is estimated to extend back nearly to the early late Eocene (so about 4 million years younger than previously; see A3). Considering the HPD associated to these estimated median ages, the lower bounds remain relatively old, thereby resulting in a substantial incompleteness of the fossil record.

Outside of the Platyrrhini clade, this BTM analysis recovers the crownward branching of the Amphipithecidae within the Anthropeida clade (Fig. S9). As in the MP A1 analysis (Fig. S5), Amphipithecidae are resolved close to the Catarrhini clade, and sister to Platyrrhini. However, these relationships have low posterior probabilities (Fig. S9) (see also results of the BTM A6 analysis below).

Contrary to the MP A1 analysis, this BTM A5 analysis recovers a better arrangement of the main families and higher-groups of known anthropoid primates from Africa (Fig. S9). Parapithecoids (including *Ucayalipithecus*) are found here as a monophyletic group (53, 121), including *Proteopithecus* and *Arsinoea*, which are both resolved as the earliest offshoots of this clade (rather than being set apart and successively arranged as in the MP A1 tree; Fig. S5). Oligopithecidae (including *Perupithecus*) are also found sister to Propithecidae (+ crown Catarrhini), rather than being successively arranged as in the MP A1 tree. Emergences of these main African anthropoid clades are also estimated to be slightly younger of about 5 million years (see Fig. S9).

Results of the A6 analysis: We performed the same BTM analysis than the A5 analysis, but in constraining the Amphipithecidae clade in a more basal position within the Anthropeida clade (i.e., stem anthropoids, diverging after the Eosimiiformes). Applying this constraint did not impact the rest of the topology (Fig. S10), which remained identical to that resulting from the A5 analysis (Fig. S9). This BTM analysis also provides divergence-time estimates of the concerned taxa that are roughly or very similar to those obtained by the A5 analysis (Table S4).

All these analyses (PAUP and the multiple BTM analyses) returned identical results regarding the eosimiid status of the new taxon, *Ashaninkacebus*. In addition, we examined the uncertainty of the phylogenetic position of *Ashaninkacebus* across the posterior trees of the BTM analyses (A5 and A6) after excluding the burn-in period, using the RoguePlots approach (122). In these two BTM analyses, *Ashaninkacebus* was not identified as a rogue taxon (i.e., it does not shift from a clade to another within Anthropeida and does not alter the global phylogeny), but instead, it was always recovered nested within the Eosimiiformes (see Figs. S11 and S12).

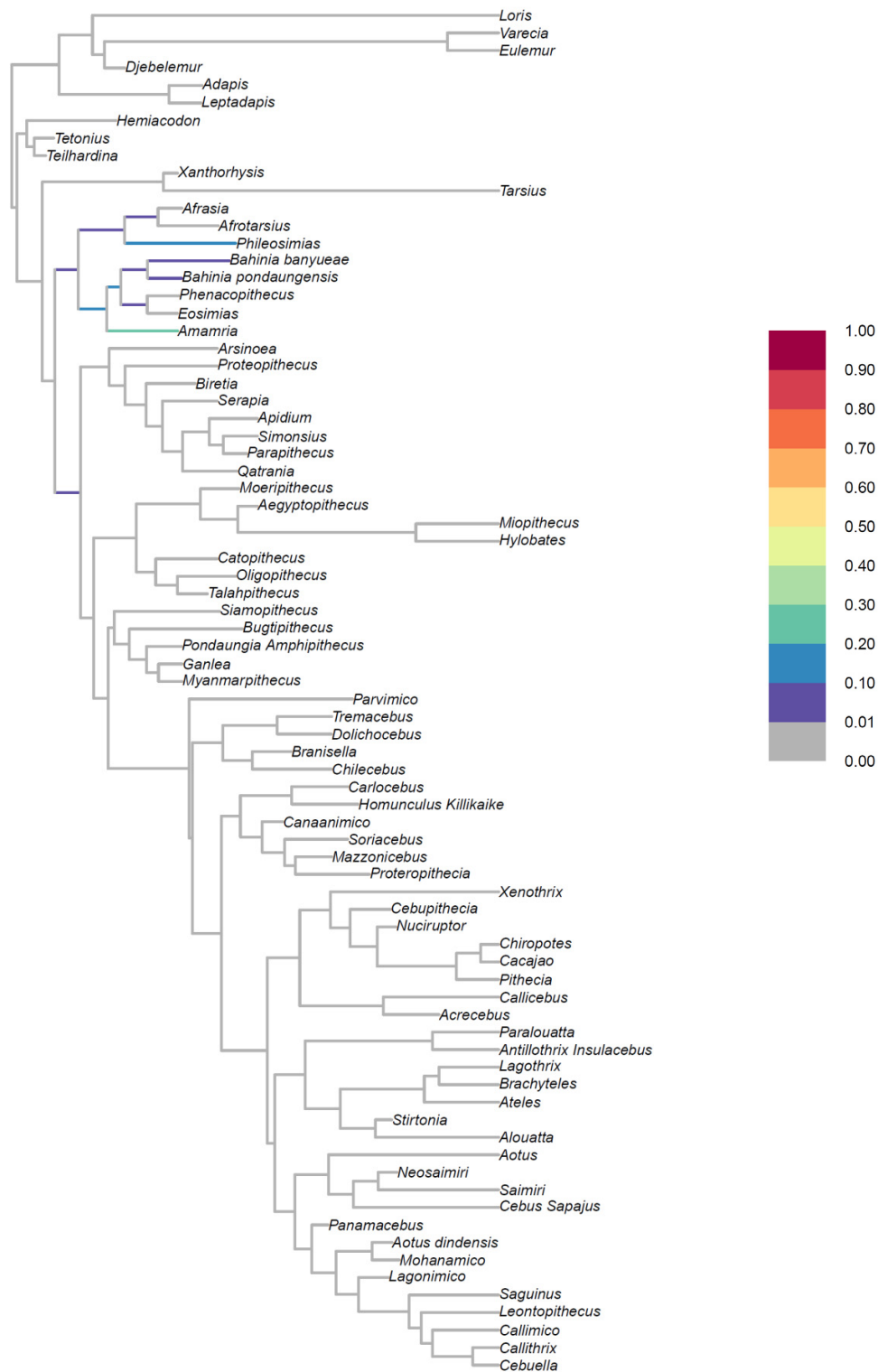


Fig. S11. RogPlots approach (122) to examine the uncertainty of the phylogenetic position of *Ashaninkacebus* across the posterior trees of the A5 BTM analysis (after excluding the burn-in period). *Ashaninkacebus* is primarily recovered nested within Eosimiiformes.

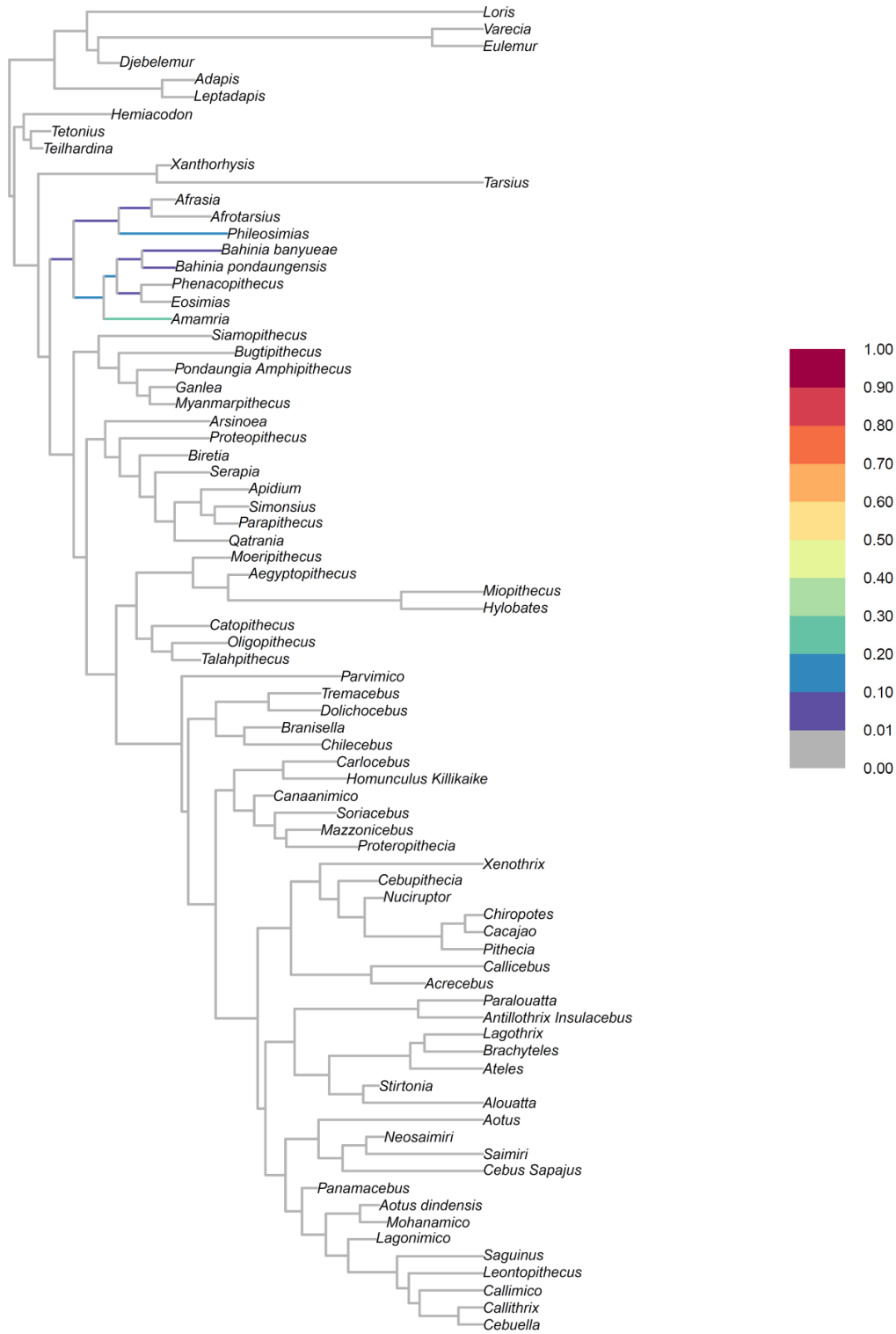


Fig. S12. RogPlots approach (122) to examine the uncertainty of the phylogenetic position of *Ashaninkacebus* across the posterior trees of the A6 BTD analysis (after excluding the burn-in period). *Ashaninkacebus* is always recovered nested within Eosimiiformes.

Text S4. Prior perturbation assessments for Bayesian tip-dating analyses (for A3).

[Run-00 – standard matrix]

```
prset brlenspr = clock:fossilization;  
prset speciationpr = exp(50.0);  
prset extinctionpr = beta(1.0,1.0);  
prset fossilizationpr = beta(1.0,1.0);  
prset treeagepr = uniform(56,60);  
prset sampleprob = 0.005;  
prset samplestrat = fossiltip;  
prset clockvarpr = igr;  
prset igrvarpr = exp(3);  
prset nodeagepr = calibrated;  
prset clockratepr = normal(0.25,0.05);
```

[Run-01]

```
prset brlenspr = clock:fossilization;  
prset speciationpr = exp(10.0);  
prset extinctionpr = beta(1.0,1.0);  
prset fossilizationpr = beta(1.0,1.0);  
prset treeagepr = uniform(56,60);  
prset sampleprob = 0.005;  
prset samplestrat = fossiltip;  
prset clockvarpr = igr;  
prset igrvarpr = exp(3);  
prset nodeagepr = calibrated;  
prset clockratepr = normal(0.25,0.05);
```

[Run-02]

```
prset brlenspr = clock:fossilization;  
prset speciationpr = exp(10.0);  
prset extinctionpr = beta(1.0,1.0);  
prset fossilizationpr = beta(1.0,1.0);  
prset treeagepr = uniform(56,60);  
prset sampleprob = 0.005;  
prset samplestrat = fossiltip;  
prset clockvarpr = igr;  
prset igrvarpr = exp(10.0);  
prset nodeagepr = calibrated;  
prset clockratepr = normal(0.25,0.05);
```

[Run-03]

```
prset brlenspr = clock:fossilization;  
prset speciationpr = exp(50.0);  
prset extinctionpr = beta(1.0,1.0);  
prset fossilizationpr = beta(1.0,1.0);  
prset treeagepr = uniform(56,60);  
prset sampleprob = 0.005;  
prset samplestrat = fossiltip;  
prset clockvarpr = igr;
```

```
prset igrvarpr = exp(10.0);  
prset nodeagepr = calibrated;  
prset clockratepr = normal(0.25,0.05);
```

[Run-04]

```
prset brlenspr = clock:fossilization;  
prset speciationpr = exp(50.0);  
prset extinctionpr = beta(1.0,1.0);  
prset fossilizationpr = beta(1.0,1.0);  
prset treeagepr = uniform(56,60);  
prset sampleprob = 0.005;  
prset samplestrat = fossiltip;  
prset clockvarpr = igr;  
prset igrvarpr = exp(3);  
prset nodeagepr = calibrated;  
prset clockratepr = normal(0.1,0.01);
```

[Run-05]

```
prset brlenspr = clock:fossilization;  
prset speciationpr = exp(50.0);  
prset extinctionpr = beta(1.0,1.0);  
prset fossilizationpr = beta(1.0,1.0);  
prset treeagepr = uniform(56,60);  
prset sampleprob = 0.005;  
prset samplestrat = fossiltip;  
prset clockvarpr = igr;  
prset igrvarpr = exp(3);  
prset nodeagepr = calibrated;  
prset clockratepr = normal(0.01,0.001);
```

Dataset S1 (separate file). Characters and character states used in the phylogenetic analysis.

Dataset S2 (separate file). Matrix for the cladistic analyses (for PAUP* 4.0a).

Dataset S3 (separate file). Matrix for the Bayesian tip-dating analysis (for MrBayes 3.2.7).

Dataset S4 (separate file). Constraints for the different Bayesian tip-dating analyses (for MrBayes 3.2.7) – A3, A4, A5 and A6 (see Table S2).

SI References

1. A. M. Ribeiro *et al.*, "Mamíferos fósiles y biocronología en el suroeste de la Amazonia, Brasil" in *El Neógeno de la Mesopotamia Argentina*, D. Brandoni, J. I. Noriega, Eds. (Asociación Paleontológica Argentina, Buenos Aires, 2013), vol. 14, pp. 207–221.
2. M. Arnal, M. E. Pérez, L. M. Tejada Medina, K. E. Campbell, The high taxonomic diversity of the Palaeogene hystricognath rodents (Caviomorpha) from Santa Rosa (Peru, South America) framed within a new geochronological context. *Hist. Biol.* **34**, 2350–2373 (2022).
3. L. Marivaux *et al.*, A morphological intermediate between eosimiiform and simiiform primates from the late middle Eocene of Tunisia: macroevolutionary and paleobiogeographic implications of early anthropoids. *Am. J. Phys. Anthropol.* **154**, 387–401 (2014).
4. F. S. Szalay, E. Delson, *Evolutionary History of the Primates* (Academic Press, New York, 1979), pp. 580.
5. L. Marivaux, The eosimiid and amphipithecoid primates (Anthropoidea) from the Oligocene of the Bugti Hills (Balochistan, Pakistan): new insight into early higher primate evolution in South Asia. *Palaeovertebrata* **34**, 29–109 (2006).
6. L. Marivaux *et al.*, Dental remains of cebid platyrrhines from the earliest late Miocene of Western Amazonia, Peru: macroevolutionary implications on the extant capuchin and marmoset lineages. *Am. J. Phys. Anthropol.* **161**, 478–493 (2016).
7. R. F. Kay, "Giant" tamarin from the Miocene of Colombia. *Am. J. Phys. Anthropol.* **95**, 333–353 (1994).
8. K. Luchterhand, R. F. Kay, R. H. Madden, *Mohanamico hershkovitzi*, gen. et sp. nov., un primate du Miocène moyen d'Amérique du Sud. *C. R. Acad. Sci., Paris* **303**, 1753–1758 (1986).
9. R. F. Kay, M. A. Cozzuol, New platyrrhine monkeys from the Solimões Formation (late Miocene, Acre State, Brazil). *J. Hum. Evol.* **50**, 673–686 (2006).
10. J. I. Bloch *et al.*, First North American fossil monkey and early Miocene tropical biotic interchange. *Nature* **533**, 243–246 (2016).
11. R. A. Stirton, Ceboid monkeys from the Miocene of Columbia. *Univ. California Pub. Geol. Sc.* **28**, 315–356 (1951).
12. M. Takai, New specimens of *Neosaimiri fieldsi* from La Venta, Colombia: a middle Miocene ancestor of the living squirrel monkeys. *J. Hum. Evol.* **27**, 329–360 (1994).
13. M. Nakatsukasa, M. Takai, T. Setoguchi, Functional morphology of the postcranium and locomotor behaviour of *Neosaimiri fieldsi*, a *Saimiri*-like middle Miocene platyrrhine. *Am. J. Phys. Anthropol.* **102**, 515–544 (1997).
14. T. Setoguchi, A. L. Rosenberger, A fossil owl monkey from La Venta, Colombia. *Nature* **326**, 692–694 (1987).
15. D. J. Meldrum, R. F. Kay, *Nuciraptor rubricae*, a new pitheciin seed predator from the Miocene of Colombia. *Am. J. Phys. Anthropol.* **102**, 407–427 (1997).
16. R. F. Kay, D. Johnson, D. J. Meldrum, A new pitheciin primate from the middle Miocene of Argentina. *Am. J. Primatol.* **45**, 317–336 (1998).
17. R. F. Kay, D. Johnson, D. J. Meldrum, Corrigendum. *Am. J. Primatol.* **47**, 347 (1999).

18. P. Hershkovitz, Notes on Tertiary platyrrhine monkeys and description of a new genus from the late Miocene of Columbia. *Folia Primatol.* **12**, 1–37 (1970).
19. T. Setoguchi, T. Watabe, T. Mouri, The upper dentition of *Stirtonia* (Ceboidea, primates) from the Miocene of Colombia, South America, and the origins of the posterointernal cusp of upper molars. *Kyoto Univ. Overseas Res. Rep. New World Monkeys* **3**, 51–60 (1981).
20. J. J. Flynn, A. R. Wyss, R. Charrier, C. C. Swisher III, An early Miocene anthropoid skull from the Chilean Andes. *Nature* **373**, 603–607 (1995).
21. R. F. Kay, "A new primate from the early Miocene of Gran Barranca, Chubut Province, Argentina: paleoecological implications" in *The Paleontology of Gran Barranca: Evolution and Environmental Change through the Middle Cenozoic of Patagonia*, R. H. Madden, A. A. Carlini, M. G. Vucetich, R. F. Kay, Eds. (Cambridge University Press, Cambridge, 2010), pp. 216–235.
22. F. Ameghino, Los monos fosiles del Eoceno de la Republica Argentina. *Rev. Arg. Hist. Nat.* **1**, 383–397 (1891).
23. F. Ameghino, Nuevos restos de mamiferos fosiles descubiertos por C. Ameghino en el Eoceno inferior de la Patagonia austral. Especies nueva, adiciones y correcciones. *Rev. Arg. Hist. Nat.* **1**, 289–328 (1891).
24. H. Bluntschli, *Homunculus patagonicus* und die ihm zugereichten Fossilfunde aus den Santa-Cruz-Schichten Patagoniens: eine morphologische Revision an Hand der Originalstucke in der Sammlung Ameghino zu La Plata. *Gen. Morphol. Jahrb.* **67**, 811–892 (1931).
25. P. Hershkovitz, Comparative anatomy of platyrrhine mandibular cheek teeth dpm4, pm4, m1 with particular reference to those of *Homunculus* (Cebidae), and comments on platyrrhine origins. *Folia Primatol.* **35**, 179–217 (1981).
26. M. F. Tejedor, A. A. Tauber, A. L. Rosenberger, C. C. Swisher, M. E. Palacios, New primate genus from the Miocene of Argentina. *Proc. Natl. Acad. Sci. U.S.A.* **103**, 5437–5441 (2006).
27. J. M. G. Perry, R. F. Kay, S. F. Vizcaino, M. S. Bargo, Oldest known cranium of a juvenile New World monkey (Early Miocene, Patagonia, Argentina): Implications for the taxonomy and the molar eruption pattern of early platyrrhines. *J. Hum. Evol.* **74**, 67–81 (2014).
28. J. G. Fleagle, D. W. Powers, G. C. Conroy, J. P. Watters, New fossil platyrrhines from Santa Cruz Province, Argentina. *Folia Primatol.* **48**, 65–77 (1987).
29. J. G. Fleagle, New fossil platyrrhines from the Pinturas Formation, Southern Argentina. *J. Hum. Evol.* **19**, 61–85 (1990).
30. F. Anapol, J. G. Fleagle, Fossil platyrrhine forelimb bones from the early Miocene of Argentina. *Am. J. Phys. Anthropol.* **76**, 417–428 (1988).
31. J. L. Kraglievich, Contribuciones al conocimiento de los primates fosil de la Patagonia. I. Diagnosis previa de un nuevo primate fosil del Oligoceno superior (Colhuehuapiano) de Gaiman, Chubut. *Comunicaciones, Inst. Nac. Invest. Cie. Nat.* **2**, 57–82 (1951).
32. J. G. Fleagle, T. M. Bown, New primate fossils from late Oligocene (Colhuehuapian) localities of Chubut Province, Argentina. *Folia Primatol.* **41**, 240–266 (1983).
33. L. A. Reeser, Morphological affinities of new fossil talus of *Dolichocebus gaimanensis*. *Am. J. Phys. Anthropol.* **63**, 206–207 (1984).
34. R. F. Kay *et al.*, The anatomy of *Dolichocebus gaimanensis*, a stem platyrrhine monkey from Argentina. *J. Hum. Evol.* **54**, 323–382 (2008).
35. P. Hershkovitz, A new genus of late Oligocene monkey (Cebidae, Platyrrhini) with notes on postorbital closure and platyrrhine evolution. *Folia Primatol.* **21**, 1–35 (1974).
36. L. Marivaux *et al.*, Neotropics provide insights into the emergence of New World monkeys: new dental evidence from the late Oligocene of Peruvian Amazonia. *J. Hum. Evol.* **97**, 159–175 (2016).
37. P.-O. Antoine *et al.*, A 60-million-year Cenozoic history of western Amazonian ecosystems in Contamana, eastern Peru. *Gondwana Res.* **31**, 30–59 (2016).
38. R. Hoffstetter, Un Primate de l'Oligocène inférieur sud-américain : *Branisella boliviana* gen. et sp. nov. *C. R. Acad. Sci., Paris* **269**, 434–437 (1969).
39. A. L. Rosenberger, A mandible of *Branisella boliviana* (Platyrrhini, Primates) from the Oligocene of South America. *Int. J. Primatol.* **2**, 1–7 (1981).
40. M. Takai, F. Anaya, New specimens of the oldest fossil platyrrhine, *Branisella boliviana*, from Salla, Bolivia. *Am. J. Phys. Anthropol.* **99**, 301–317 (1996).

41. M. Takai, F. Anaya, N. Shigehara, T. Setoguchi, New fossil materials of the earliest New World Monkey, *Branisella boliviana*, and the problem of platyrrhine origins. *Am. J. Phys. Anthropol.* **111**, 263–281 (2000).
42. R. D. E. MacPhee, C. A. Woods, A new fossil cebine from Hispaniola. *Am. J. Phys. Anthropol.* **58**, 419–436 (1982).
43. R. D. E. MacPhee, I. Horovitz, O. Arredondo, O. Jiménez Vázquez, A new genus for the extinct Hispaniolan monkey *Saimiri bernensis* Rímoli, 1977, with notes on its systematic position. *Am. Mus. Novitates* **3134**, 1–21 (1995).
44. S. B. Cooke, A. L. Rosenberger, S. Turvey, An extinct monkey from Haiti and the origins of the Greater Antillean primates. *Proc. Natl. Acad. Sci. U.S.A.* **108**, 2699–2704 (2011).
45. A. L. Rosenberger, S. B. Cooke, R. Rimoli, X. Ni, L. Cardoso, First skull of *Antillothrix bernensis*, an extinct relict monkey from the Dominican Republic. *Proc. Royal Soc. B* **278**, 67–74 (2011).
46. M. Rivero, O. Arredondo, *Paralouatta varonai*, a new Quaternary platyrrhine from Cuba. *J. Hum. Evol.* **21**, 1–11 (1991).
47. I. Horovitz, R. D. E. MacPhee, The Quaternary Cuban platyrrhine *Paralouatta varonai* and the origin of Antillean monkeys. *J. Hum. Evol.* **36**, 33–68 (1999).
48. E. E. Williams, K. F. Koopman, West Indian fossil monkeys. *Am. Mus. Novitates* **1546**, 1–16 (1952).
49. R. D. E. MacPhee, I. Horovitz, New craniodental remains of the Quaternary Jamaican monkey *Xenothrix mcgregori* (Xenotrichini, Callicebinae, Pitheciidae), with a reconsideration of the *Aotus* hypothesis. *Am. Mus. Novitates* **3434**, 1–51 (2004).
50. R. F. Kay *et al.*, *Parvimico materdei* gen. et sp. nov.: a new platyrrhine from the Early Miocene of the Amazon Basin, Peru. *J. Hum. Evol.* **134**, 102628 (2019).
51. M. Bond *et al.*, Eocene primates of South America and the African origins of New World monkeys. *Nature* **520**, 538–541 (2015).
52. K. E. Campbell Jr, P. B. O'Sullivan, J. G. Fleagle, D. De Vries, E. R. Seiffert, An Early Oligocene age for the oldest known monkeys and rodents of South America. *Proc. Natl. Acad. Sci. U.S.A.* **118**, e2105956118 (2021).
53. E. R. Seiffert *et al.*, A parapithecoid stem anthropoid of African origin in the Paleogene of South America. *Science* **368**, 194–197 (2020).
54. E. L. Simons, New fossil apes from Egypt and the initial differentiation of Hominoidea. *Nature* **205**, 135–139 (1965).
55. E. L. Simons, New faces of *Aegyptopithecus* from the Oligocene of Egypt. *J. Hum. Evol.* **16**, 273–290 (1987).
56. R. F. Kay, J. G. Fleagle, E. L. Simons, A revision of the Oligocene apes of the Fayum Province, Egypt. *Am. J. Phys. Anthropol.* **55**, 293–322 (1981).
57. F. Ankel-Simons, J. G. Fleagle, P. S. Chatrath, Femoral anatomy of *Aegyptopithecus zeuxis*, an early Oligocene anthropoid. *Am. J. Phys. Anthropol.* **106**, 413–424 (1998).
58. H. Thomas, S. Sen, J. Roger, Z. Al-Sulaimani, The discovery of *Moeripithecus markgrafi* Schlosser (Propliopithecidae, Anthroipoidea, Primates), in the Ashawq Formation (early Oligocene of Dhofar Province, Sultanate of Oman). *J. Hum. Evol.* **20**, 33–49 (1991).
59. E. Simons, Description of two genera and species of Late Eocene Anthroipoidea from Egypt. *Proc. Natl. Acad. Sci. U.S.A.* **86**, 9956–9960 (1989).
60. E. L. Simons, Discovery of the oldest known anthropoidean skull from the Paleogene of Egypt. *Science* **247**, 1567–1569 (1990).
61. E. L. Simons, Skulls and anterior teeth of *Catopithecus* (Primates, Anthroipoidea) from the Eocene and anthropoid origins. *Science* **268**, 1885–1888 (1995).
62. E. L. Simons, D. T. Rasmussen, Skull of *Catopithecus browni*, an early Tertiary catarrhine. *Am. J. Phys. Anthropol.* **100**, 261–292 (1996).
63. E. L. Simons, Two new primate species from the African Oligocene. *Postilla* **64**, 1–12 (1962).
64. D. T. Rasmussen, E. L. Simons, New specimens of *Oligopithecus savagei*, early Oligocene primate from the Fayum, Egypt. *Folia Primatol.* **51**, 182–208 (1988).
65. E. Gheerbrant, H. Thomas, S. Sen, Z. Al-Sulaimani, Nouveau Primate Oligopithecinae (Simiiformes) de l'Oligocène inférieur de Taqah, Sultanat d'Oman. *C. R. Acad. Sci., Paris* **321**, 425–432 (1995).

66. J.-J. Jaeger *et al.*, Late middle Eocene epoch of Libya yields earliest known radiation of African anthropoids. *Nature* **467**, 1095–1098 (2010).
67. E. L. Simons, Diversity in the early Tertiary anthropoidean radiation in Africa. *Proc. Natl. Acad. Sci. U.S.A.* **89**, 10743–10747 (1992).
68. E. L. Simons, Preliminary description of the cranium of *Proteopithecus sylviae*, an Egyptian Late Eocene anthropoidean primate. *Proc. Natl. Acad. Sci. U.S.A.* **94**, 14970–14975 (1997).
69. E. R. Miller, E. L. Simons, Dentition of *Proteopithecus sylviae*, an archaic anthropoid from Fayum, Egypt. *Proc. Natl. Acad. Sci. U.S.A.* **94**, 13760–13764 (1997).
70. E. L. Simons, E. R. Seiffert, A partial skeleton of *Proteopithecus sylviae* (Primates, Anthropoidea): first associated dental and postcranial remains of an Eocene anthropoidean. *C. R. Acad. Sci., Paris* **329**, 921–927 (1999).
71. L. Bonis de, J.-J. Jaeger, B. Coiffait, P.-E. Coiffait, Découverte du plus ancien primate catarrhinien connu dans l'Éocène supérieur d'Afrique du Nord. *C. R. Acad. Sci.* **306**, 929–934 (1988).
72. E. R. Seiffert *et al.*, Basal anthropoids from Egypt and the antiquity of Africa's higher primate radiation. *Science* **310**, 300–304 (2005).
73. E. Simons, R. F. Kay, *Qatrania*, new basal anthropoid primate from the Fayum, Oligocene of Egypt. *Nature* **304**, 624–626 (1983).
74. E. Simons, R. F. Kay, New material of *Qatrania* from Egypt with comments on the phylogenetic position of the Parapithecidae (primates, Anthropoidea). *Am. J. Phys. Anthropol.* **15**, 337–347 (1988).
75. M. Schösser, Beiträge zur Kenntnis der oligozänen Landsäugetiere aus dem Fayum, Ägypten. *Beit. Paläontol. Geol. Österreich-Ungarns* **24**, 51–167 (1911).
76. E. L. Simons, *Parapithecus grangeri* (Parapithecidae, Old World higher primates): new species from the Oligocene of Egypt and the initial differentiation of Cercopithecoidea. *Postilla* **166**, 1–12 (1974).
77. E. L. Simons, *Parapithecus grangeri* of the African Oligocene: an archaic catarrhine without lower incisors. *J. Hum. Evol.* **15**, 205–213 (1986).
78. E. L. Simons, The cranium of *Parapithecus grangeri*, an Egyptian Oligocene anthropoidean primate. *Proc. Natl. Acad. Sci. U.S.A.* **98**, 7892–7897 (2001).
79. H. F. Osborn, New fossil mammals from the Fayûm Oligocene, Egypt. *Am. Mus. Nat. Hist. Bull.* **26**, 415–424 (1908).
80. J. G. Fleagle, E. L. Simons, Limb skeleton and locomotor adaptations of *Apidium phiomense*, an Oligocene anthropoid from Egypt. *Am. J. Phys. Anthropol.* **97**, 235–289 (1995).
81. M. Takai *et al.*, A new anthropoid from the latest middle Eocene of Pondaung, Central Myanmar. *J. Hum. Evol.* **40**, 393–409 (2001).
82. K. C. Beard *et al.*, A new primate from the Eocene Pondaung Formation of Myanmar and the monophyly of Burmese amphipithecids. *Proc. Royal Soc. B* **276**, 3285–3294 (2009).
83. J.-J. Jaeger *et al.*, Amphipithecine primates are stem anthropoids: cranial and postcranial evidence. *Proc. Royal Soc. B* **287**, 20202129 (2020).
84. E. H. Colbert, A new primate from the upper Eocene Pondaung Formation of Burma. *Am. Mus. Novitates* **651**, 1–18 (1937).
85. Y. Chaimanee *et al.*, A lower jaw of *Pondaungia cotteri* from the Late Middle Eocene Pondaung Formation (Myanmar) confirms its anthropoid status. *Proc. Natl. Acad. Sci. U.S.A.* **97**, 4102–4105 (2000).
86. R. L. Ciochon, G. F. Gunnell, Eocene primates from Myanmar: historical perspectives on the origin of Anthropoidea. *Evol. Anthropol.* **11**, 156–168 (2002).
87. R. L. Ciochon, G. F. Gunnell, "Eocene large-bodied primates of Myanmar and Thailand: morphological considerations and phylogenetic affinities" in *Anthropoid Origins: New Visions*, C. F. Ross, R. F. Kay, Eds. (Plenum, New York, 2004), pp. 249–282.
88. P. Coster *et al.*, Uniquely derived upper molar morphology of Eocene Amphipithecidae (Primates: Anthropoidea): homoplasy and phylogeny. *J. Hum. Evol.* **65**, 143–155 (2013).
89. Y. Chaimanee, V. Suteethorn, J.-J. Jaeger, S. Ducrocq, A new late Eocene anthropoid primate from Thailand. *Nature* **385**, 429–431 (1997).

90. Y. Chaimanee, S. Khansubha, J.-J. Jaeger, A new lower jaw of *Siamopithecus eocaenus* from the Late Eocene of Thailand. *C. R. Acad. Sci. Vie, Paris* **323**, 235–241 (2000).
91. S. Ducrocq, *Siamopithecus eocaenus*, a late Eocene anthropoid primate from Thailand: its contribution to the evolution of anthropoids in Southeast Asia. *J. Hum. Evol.* **36**, 613–635 (1999).
92. C. P. E. Zollikofer *et al.*, The face of *Siamopithecus*: new geometric-morphometric evidence for its anthropoid status. *Anat. Rec.* **292**, 1734–1744 (2009).
93. L. Marivaux *et al.*, Anthropoid primates from the Oligocene of Pakistan (Bugti Hills): data on early anthropoid evolution and biogeography. *Proc. Natl. Acad. Sci. U.S.A.* **102**, 8436–8441 (2005).
94. K. C. Beard, T. Qi, M. R. Dawson, B. Wang, C. Li, A diverse new primate fauna from middle Eocene fissure-fillings in southeastern China. *Nature* **368**, 604–609 (1994).
95. K. C. Beard, Y. Tong, M. R. Dawson, J. Wang, X. Huang, Earliest complete dentition of an anthropoid primate from the late middle Eocene of Shanxi Province, China. *Science* **272**, 82–85 (1996).
96. Y. Tong, *Middle Eocene small mammals from Liguanqiao Basin of Henan Province and Yuanqu Basin of Shanxi Province, Central China*. T. C. A. o. Sciences, Ed. (Paleontogia Sinica, Beijing, ed. Sciences Press, 1997), vol. 186 (26), pp. 256.
97. K. C. Beard, J. Wang, The eosimiid primates (Anthropoidea) of the Heti Formation, Yuanqu Basin, Shanxi and Henan Provinces, People's Republic of China. *J. Hum. Evol.* **46**, 401–432 (2004).
98. J.-J. Jaeger *et al.*, A new primate from the middle Eocene of Myanmar and the Asian early origin of anthropoids. *Science* **286**, 528–530 (1999).
99. X. Ni, Q. Li, L. Li, K. C. Beard, Oligocene primates from China reveal divergence between African and Asian primate evolution. *Science* **352**, 673–677 (2016).
100. E. L. Simons, T. M. Bown, *Afrotarsius chatrathi*, first tarsiform primate (? Tarsiidae) from Africa. *Nature* **313**, 475–477 (1985).
101. Y. Chaimanee *et al.*, A new middle Eocene primate from Myanmar and the initial anthropoid colonization of Africa. *Proc. Natl. Acad. Sci. U.S.A.* **109**, 10293–10297 (2012).
102. K. C. Beard, "A new genus of Tarsiidae (Mammalia: Primates) from the middle Eocene of Shanxi Province, China, with notes on the historical biogeography of tarsiers" in *Dawn of the Age of Mammals in Asia*, K. C. Beard, M. R. Dawson, Eds. (*Bull. Carnegie Mus. Nat. Hist.*, Pittsburgh, 1998), vol. 34, pp. 260–277.
103. P. Teilhard de Chardin, Les mammifères de l'Éocène inférieur de la Belgique. *Mém. Mus. Roy. Hist. Nat. Belgique* **36**, 1–33 (1927).
104. O. C. Marsh, Preliminary description of new Tertiary mammals. I–IV. *Am. J. Sci.* **4**, 22–28, 202–224 (1872).
105. W. D. Matthew, A revision of the lower Eocene Wasatch and Wind River faunas. IV. Entelonychia. *Bull. Am. Mus. Nat. Hist.* **34**, 429–483 (1915).
106. H. Filhol, Nouvelles observations sur les mammifères des gisements de phosphates de chaux (Lémuriens et Pachylémuriens). *Ann. Sc. Géol.* **5**, 1–36 (1874).
107. P. Gervais, *Zoologie et Paléontologie Générale, 2nd Edition*. (Bertrand, Paris, 1876).
108. G. Cuvier, *Discours sur la théorie de la Terre, servant d'introduction aux recherches sur les ossements fossiles* (Paris, 1821).
109. J.-L. Hartenberger, B. Marandat, A new genus and species of an early Eocene Primate from North Africa. *Human. Evol.* **7**, 9–16 (1992).
110. L. Marivaux *et al.*, *Djebelémur*, a tiny pre-tooth-combed primate from the Eocene of Tunisia: a glimpse into the origin of crown strepsirhines. *PLoS ONE* **8**, 1–21 (2013).
111. H. Sauquet, A practical guide to molecular dating. *C. R. Palevol* **12**, 355–367 (2013).
112. S. Y. W. Ho, *The Molecular Evolutionary Clock. Theory and Practice*. S. Y. W. Ho, Ed. (Springer, Cham, 2020).
113. R. Zaragüeta Bagils, H. Lelièvre, P. Tassy, Temporal paralogy, cladograms, and the quality of the fossil record. *Geodiversitas* **26**, 381–389 (2014).
114. P. Tassy, "The making of Paleontological time. Philosophical Perspectives of Time in Natural Sciences" in *Time of Nature and the Nature of Time*, C. Bouton, P. Huneman, Eds. (Springer, Cham, 2017), vol. 326, pp. 253–271.

115. R. F. Kay, Biogeography in deep time - What do phylogenetics, geology, and paleoclimate tell us about early platyrrhine evolution? *Mol. Phylogenet. Evol.* **82**, 358–374 (2015).
116. R. Woods, S. T. Turvey, S. Brace, R. D. E. MacPhee, I. Barnes, Ancient DNA of the extinct Jamaican monkey *Xenothrix* reveals extreme insular change within a morphologically conservative radiation. *Proc. Natl. Acad. Sci. USA* **115**, 12769–12774 (2018).
117. L. Marivaux *et al.*, Talar morphology, phylogenetic affinities and locomotor adaptation of a large-bodied amphipithecoid primate from the late middle Eocene of Myanmar. *Am. J. Phys. Anthropol.* **143**, 208–222 (2010).
118. Y. Chaimanee, O. Chavasseau, V. Lazzari, A. Euriat, J.-J. Jaeger, A new Late Eocene primate from the Krabi Basin (Thailand) and the diversity of Palaeogene anthropoids in southeast Asia. *Proc. Royal Soc. B* **280**, 1471–2954 (2013).
119. J.-J. Jaeger *et al.*, New Eocene primate from Myanmar shares dental characters with African Eocene crown anthropoids. *Nat. Commun.* **10**, 3531 (2019).
120. K. C. Beard, *The hunt for the dawn monkey. Unearthing the origins of monkeys, apes, and humans* (University of California Press, Berkeley, 2004).
121. E. R. Seiffert, Early primate evolution in Afro-Arabia. *Evol. Anthropol.* **21**, 239–253 (2012).
122. S. Klopstein, T. Spasojevic, Illustrating phylogenetic placement of fossils using RoguePlots: An example from ichneumonid parasitoid wasps (Hymenoptera, Ichneumonidae) and an extensive morphological matrix. *PLoS ONE* **14**, e0212942 (2019).